Doctoral Dissertation

The 80 years geochemical records in Porites coral from Con Dao island, Viet Nam as an indicator for Mekong river discharge and monsoon climate variability

(ベトナム Con Dao 島のハマサンゴ骨格の地球化学指標に記録される過去 80 年間のメコン川の流出とモンスーン気候の変動)

Phan Thanh Tung

2019/03

List of figures and tables

Figure 3.1. (a) Location of the East Sea and Mekong River of Vietnam. The climate of this area is strongly dominated by the East Asian monsoon: summer monsoon and winter monsoon correspond to southwesterly winds and northeasterly winds, respectively. Con Dao Island located in the ESVN, ~ 90 km from the mouth of the Mekong River. (b) Map of Con Dao Island showing the location of the sampling site at the southwest side of the island (red circle). Meteorological observation station (blue circle) located 15 km distance away from the sampling site.

Figure 3.2. X-radiograph (top) and UV-luminescence photograph (bottom) of a coral skeletal core slab (Porites sp.) from Con Dao Island showing annual bands for AD 1922 - 2005. The UV photograph and X-ray photograph revealed clear luminescent banding and density banding in the coral, respectively. One year is represented by high-density/low-density couplet. The red lines indicate the measurement lines for geochemical analysis. The scale bars are 30 cm.

Figure 3.3. Comparison between geochemical records of Porites coral from Con Dao Island and monthly climate data recorded by a meteorological observation station in Con Dao Island during the period from 1980 to 2005. (a) Coral skeletal Sr/Ca ratio record, (b) coral skeletal $\delta^{18}O_c$ record, (c) calculated $\delta^{18}O_{sw}$, (d) coral skeletal Ba/Ca ratio, (e) SST, (f) SSS and (g) precipitation. Red arrows indicate the years that big floods occurred.

Figure 3.4. Seasonal characteristics of (a) Sr/Ca ratios and $\delta^{18}O_{coral}$; (b) Calculated $\delta^{18}O_{seawater}$ and Ba/Ca ratio and climatological data calculated from monthly data; (c) SST and SSS and (d) precipitation in the period from 1980 to 2005. Error bars indicate standard error.

Figure 3.5. The comparison between monthly averages of calculated (a) δ18Oseawater and (b) Ba/Ca ratios during the period from 1980 to 2005, separated into flood years and no-flood years. Error bars indicate standard error.

Figure 3.6. (a) Linear least squares regression of the Sr/Ca ratio and SST for Porites coral in Con Dao Island using only annual extreme values (red circles) over the period from 1980 to 2005. Black circles are all measured values. (b) A compilation of Sr/Ca - SST thermometer readings in Porites corals from different areas. This study shows a similar slope with other studies.

Figure 3.7. Map of China seas and the neighboring region. The red ellipses or circles schematically illustrate the dimensional structure of the cold eddy locations of the major upwelling regions (Hu and Wang, 2016)

Figure 3.8. Suspended sediment transportation in the Mekong River, with a) representing for the high discharge season (southwest monsoon), b) representing for the low discharge season (northeast monsoon). Purple circles indicate erosion, yellow areas indicate deposition. Black arrows show the near surface pathways of sediment, dashed arrows show the near bottom transports of sediment.

Figure 4.1. Variation of coral Ba/Ca record from Con Dao island during period from 1924 to 2005. The peaks typically occur in Winter (December to April) and sometimes in Summer mainly August to September when flood events usually occur in Mekong Delta. Red arrows indicate possible occurred flood events (1924 to 1979) and history-based occurred flood events (1980 to 2005)

Table of contents

ACKNOWLEDGEMENT

First of all, I would like to express my sincere gratitude to my advisors Dr. Watanabe Tsuyoshi and Dr. Atsuko Yamazaki for their guidance, supervision and mentorship during the development of this study at the Hokkaido University in last three years. I am extremely grateful for encouraging my research and allowing me to grow as a research scientist. Your advice on both research as well as on my career have been invaluable. In addition, I'd like to send my great thank to Prof. Chuan-Chou Shen, Dr. Hong-Wei Chiang (National Taiwan of University) and Dr. Lam Dinh Doan (Vietnam Academy of Science and Technology) for helping me in collecting coral cores from Con Dao island and giving me some useful advices for my research.

I would also like to thank my committee members, professor Suzuki Noriyuki, professor Toru Takeshita for serving as my committee members. Thank you for your brilliant comments and suggestions.

Many thanks to all of 5G members and CREES members (Hokkaido University) for dicussions and supporting me. Special thanks to Takaaki Watanabe, Saori Ito, Taro Komagoe (CREES) who taught and supported me in using some machines for my experiments. I also want to say thank to ICP OES and MAT 253 laboratory (Hokkaido University) for facilitating me in experiments.

Let me take this opportunity to express my gratitude to MEXT scholarship and Graduate shool of Sciences for their financial sponsorship for my study. I'd like to show my appreciation to Vietnam National University, University of Science, Hanoi for their support during my time abroad.

My greatest appreciation goes to my family for their immense support and encouragement. Deepest thanks go to my Vietnamese friends for their always being with me and making my time in Sapporo memorable.

Abstract

The Mekong River is one of the most important river systems in the world, politically, economically, and environmentally. It is originated from Tibetan Plateau, flow through six countries, China, Myanmar, Laos, Thailand, Cambodia, and Viet Nam before reaching to Mekong Delta in East Sea Viet Nam (ESVN). Mekong River and ESVN are strongly dominated by the seasonal reversing of East Asian Monsoon (EAM) which causes strong seasonal climatic variations. Instrumental records of past climate variations and paleoclimatic history of Mekong river are temporally short (20–30 years), and geographically constrained, limiting our ability to examine long-term climate fluctuations. In order to resolve and reconstruct past climate variations, EAM variabilities and Mekong River discharge, the geochemical records of marine carbonates such as scleractinian corals can be used. The coral cores were collected from the colony of *Porites sp.* alive at ~20m water depth on the southwest side of Con Dao island, south of ESVN and about 90 km distance from Mekong river mouth. We measured Sr/Ca and Ba/Ca ratios using inductively coupled plasma atomic emission spectrometry (ICP-AES) and oxygen and carbon stable isotope ratios using an automated carbonate preparation device (Kiel IV) coupled to stable isotope ratio mass spectrometer (Thermo scientific MAT 253) installed at Hokkaido University. All geochemical proxies were measured in monthly resolution during the period 1924 – 2005.

The results showed the high correlation between Sr/Ca and instrumental SST ($r = 0.90$; $P < 0.01$). The differences between the reconstructed and observed SSTs were 0.45, -0.89 and -0.33 °C for annual maximum, minimum and mean values, respectively. The reconstructed SST in period from 1924 to 2005 is quite stable and the standard deviation of residuals of the regression was determined to be 1.45 °C due to differences in ocean conditions and SST between observation site and sampling site. For determining ENSO variability and its impacts to ESVN, I compared between coral Sr/Ca and Nino 3.4 index. I found that coral Sr/Ca ratios from 1924 to 1990 showed significantly correlation with Nino 3.4 index with correlation coefficient $r = 0.516$ and $r = 0.725$ corresponding to winter and summer, respectively. This result suggested that interannual variability SST around Con Dao island is strongly influenced by ENSO. From 1990 to 2005, relationship between Nino 3.4 index and summer Sr/Ca are almost opposite due to influence of Mekong river discharge or the eruption of Mount Pinatubo, Philippines.

The time series of Ba/Ca is characterized with intra-annual double peaks, the first large one in March during the dry season and relatively small one in August during the wet season. Coral Ba/Ca record in Con Dao Island could reflect the sediment discharge from the Mekong River. The maximum discharge of freshwater from the river reached our coral site in summer (from May to November), however the sediment discharge model of the Mekong River indicated that the amount of suspended sediment influencing on Con Dao Island was high in winter (from December to April) because of the influence from the seasonal migration of the Asian monsoon and ocean currents. Coral Ba/Ca ratios can be used as reflection of the suspended sediment discharge from Mekong river in period 1924 to 2005 and divided into 3 stages: Before war (1924 to 1945), Indochina war (1946 to 1975) and After war and hydropower dams construction (1976 – 2005).

The variability of Ba/Ca can be explained by human activities such as: land-use changes, hydropower dams construction and Indochina war.

On the other hand, coral Ba/Ca ratio and $\delta^{18}O_{sw}$ could be used as indicators of flooding from the Mekong Delta. During the period from 1980 to 2005, the difference in seasonal characteristics of geochemical signals in flood years and no-flood years was detected. During the flood years, in the warm/wet season, the Ba/Ca ratios and $\delta^{18}O_{sw}$ data significantly increased and decreased, respectively. These results reflect the increase in the Mekong River freshwater discharge and the sudden increase of precipitation when floods occurred in warm/wet season. In period from 1980 to 2005, the averaged value of Ba/Ca ratios in summer months (May to November) of flood years was calculated as 3.6 µmol/mol. Based on this, 11 flood events can be detected by averaged value of Ba/Ca in summer months similar or higher than 3.6 µmol/mol in 1926, 1930, 1933, 1935, 1948, 1952, 1960, 1961, 1975, 1976, and 1978, especially expected big flood events in 1948 and 1960 with averaged Ba/Ca is 4.23 and 4.25 µmol/mol, respectively.

Ba/Ca ratios and $\delta^{18}O_{sw}$ recorded by *Porites* coral in Con Dao island can be used as proxy for northeast and southwest monsoon, respectively. $\delta^{18}O_{sw}$ showed a high correlation with $\delta^{18}O$ in coral from Koshiki island which is also influenced by East Asian Monsoon. I found the significant correlation between $\delta^{18}O_{sw}$ and Pacific Decadal Oscillation (PDO) index, suggested that climate of ESVN was teleconnected with decadal variation of Pacific Ocean during the last 80 years. High correlation between summer $\delta^{18}O_{sw}$ and winter PDO index during 1924 to 1990 indicated that EASM may be a possible driving force of winter PDO variability. The no correlation between summer $\delta^{18}O_{sw}$ and winter PDO index from 1990 to 2005 corresponds with cooling event showed in the results of Sr/Ca variation.

In conlusion, the geochemical data from Porites coral of Con Dao island, Viet Nam provided a better understanding about interannual variability of sea surface conditions, Mekong river discharge and flood events determination during period from 1924 to 2005. Moreover, the interaction between ENSO and East Asian monsoon and their impacts to East sea Viet Nam were also clarified partly.

Chapter 1.
INTRODUCTION

1. East Asian monsoon

The East Asian monsoon is characterized by a distinct seasonal reversal of monsoon flow driven by temperature differences between the Pacific Ocean and East Asian continent. Because of these distinct differences, the annual cycle of the East Asian monsoon can be divided into warm, wet summer, and cold, dry winter, monsoons: this division is related to the seasonal reversal of large-scale atmospheric heating and steady circulation features (Chang, 2004; Wang, 2006). the East Asian monsoon strongly influences the global climate system and prediction. The East Asian monsoon system is much more complicated than other individual global monsoon systems because the East Asian monsoon is located in the subtropics, while the other monsoons are located in the tropics. The East Asian monsoon is influenced by mid-latitude disturbances and convective activity to represent the meridional transports of heat and momentum, in addition to significant land–sea contrast. Moreover, the East Asian monsoon system is linked to the Arctic effect and some feedbacks to the other regional tropical monsoons of the global monsoon system (Kwon et al., 2005; Lee et al., 2005).

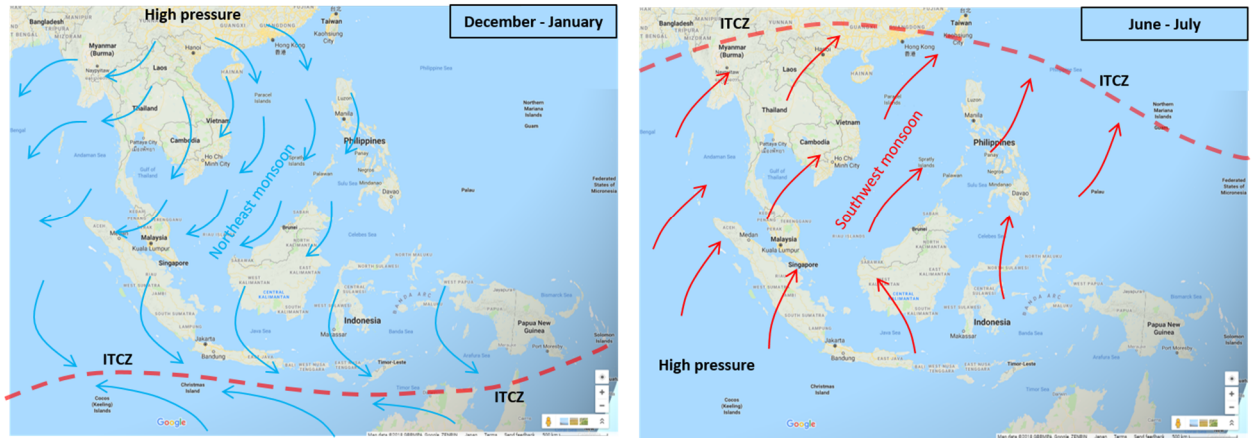

Figure 1.1. East Asian monsoon climate characterized with Southwest monsoon and Northeast monsoon

2. Mekong River basin and climate variability

The Mekong River is one of the largest river systems in the world, rises in Tibet and flows 4600 km from its source before draining into the East sea of Viet Nam. The area of the Mekong River basin is about 8.0×105 km^2 and extends into six countries: China (21%), Myanmar (3%), Thailand (23%), Laos (25%), Cambodia (20%), and Vietnam (8%). Annual water discharge from the river is tenth largest in the world with 475 km^3 (Lu and Siew, 2005), in which Laos contributes some 35% of this water, followed by Thailand and Cambodia (18% each), China (16%), Vietnam (11%) and Myanmar (2%). The annual sediment discharge of Mekong River is $1.6×10^8$ tons (Milliman and Syvitski, 1992), ninth largest in the world. The Mekong River basin can be divided into two parts: the "upper Mekong basin" in Tibet of China and small part of Myanmar, and the "lower Mekong basin" from Yunnan downstream, China to the East sea of Viet Nam, including:

Laos, Cambodia, Thailand and Viet Nam. The Upper and Lower basins make up 24 and 76 percent respectively of the total area of the basin (MRC, 2005). The Mekong Basin is particularly rich in biodiversity. The Mekong river basin is a diverse region with population of 70 million people and 70% of the basin's population rely on agriculture and fisheries for their livelihoods.

Mekong River basin is strongly dominated by East Asian monsoon with two distinct seasons – a wet season from May to November and a generally dry season for the rest of the year corresponding to southwest monsoon and northeast monsoon, respectively. In the lower Mekong river basin, the southwest monsoon brings high rainfall resulting in the onset of the rainy or wet season while the northeast monsoon has low rainfall and forms the dry season. Air temperature is remarkably uniform due to the area's maritime infl uence and generally low elevation. High temperatures occur except during part of the northeast monsoon when cool winds blow from Central Asia. Lowest temperatures occur between November and February (MRC, 2003). The hottest months are at the beginning of the dry season with average air temperatures of 30-38°C.

Precipitation in the region varies with location. Rainfall is low on the Tibet Plateau and increases southwards through the Mekong River basin, being the highest in the Mekong Delta of Viet Nam. The rainfall ranges from 600 to 3200 mm per year. Cyclonic disturbances during the rainy season may cause widespread rainfall of long duration during July-September, resulting in flooding (Chu et al. 2003). With the onset of the southwest monsoon in May, the level of the Mekong River rises reaching its peak in mid-August or early September in the upper part of the lower Mekong river basin, and in mid-September or early October in the Mekong Delta (MRC, 2003). Flooding in the Cambodian and Vietnamese parts of the Mekong river basin is usually disastrous with up to 4 million ha of Cambodia's lowland areas and up to 1.8 million ha in the Mekong Delta inundated annually.

Figure 1.2. Mekong River basin map (*Source: FAO 2011*)

3. Geochemical records from corals as proxies for paleoclimate and paleoenvironment

Tropical coral reefs are complicated ecosystems that have existed in tropical and subtropical Oceans for millions of years. Their distribution is mainly at shallow warm water regions. During their growth, massive corals incorporate a large array of geochemical elements into their aragonitic skeleton and form varying density bands that have been demonstrated to follow the annual cycles of key environmental parameters. When coral cores were cut into 5-10

mm slices along the vertical growth axis, these couples of annual density band are apparent on X-radiographs, which make these massive coral skeletons record of past tropical climates and environments significantly. In comparison with other climate records (i.e., tree rings, ice cores, sediment cores) massive corals have several characteristics that make them unique marine proxies:

- Annual density bands enable absolute chronological control
- Rapid and continuous growth (~1cm/yr) allow for annual and subseasonal sampling resolution
- Growth of several meter high colonies provide coral records of several decades up to centuries.
- The large of geochemical tracers incorporated into the aragonite skeleton reflects environmental conditions of the ambient seawater in which the coral grew.
- Main oceanographic parameters such as sea surface temperature (SST) and salinity (SSS) can be reconstructed from the coral skeleton.
- Good preserved fossil coral skeleton allows for high-resolution paleoclimate reconstruction.

The coral-based paleoclimatology benefits in order to reconstruct important oceanographic parameters such as SST and SSS at high temporal resolution. The climate reconstruction for a long time has significantly improved our understanding of the variability of the tropical and subtropical climate system.

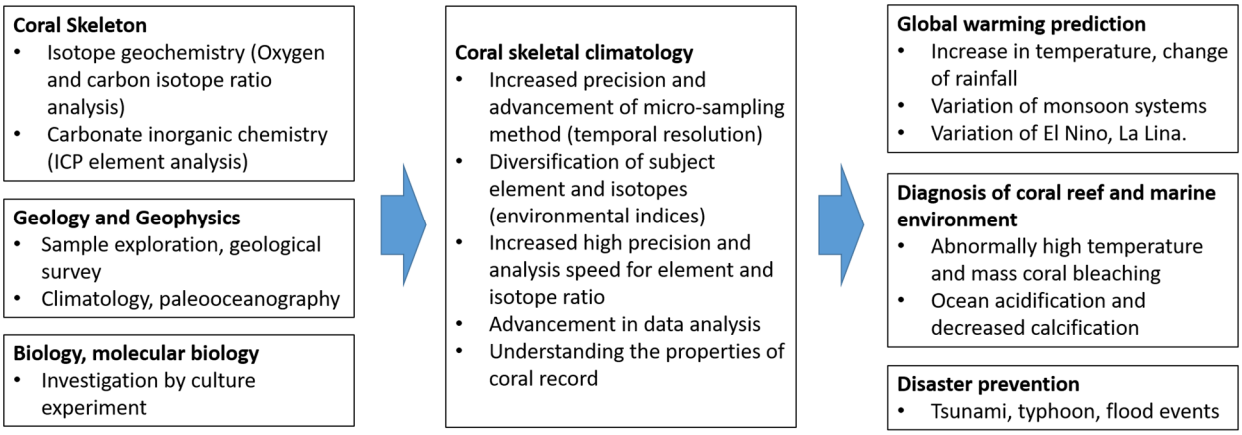

Figure 1.3. Scheme of research development for coral skeletal climatology

Proxy	Environmental variable
$\delta^{18}O$	Sea surface temperature, sea surface salinity
$\delta^{13}C$	Light intensity, nutrients/ zooplankton levels
$\Delta^{14}C$	Ocean ventilation, water mass circulation
Sr/Ca	Sea surface temperature
Mg/Ca	Sea surface temperature
U/Ca	Sea surface temperature
Mn/Ca	Wind anomalies, upwelling
Cd/Ca	Upwelling
$\delta^{11}B$	pH

F	Sea surface temperature
Ba/Ca	Upwelling, river outflow, sea surface temperatures
Skeletal growth bands	Light (seasonal changes), stress, water motion, sedimentation, sea surface temperature
Fluorescence	River outflow

Table 1.1. *Environmental variables that can be reconstructed from coral skeletal isotopes, minor elements, trace elements and growth record. Some variables, such as SST, SSS and upwelling associate more directly to ENSO*

2.1. Coral Sr/Ca ratio, a temperature proxy

Sea surface temperature (SST) is one of the most important environmental parameters influence on regional and global climate variability, and therefore it is one of the most important oceanographic parameters for predicting future climate scenarios through numerical simulations. Trace elements (i.e., Sr, Mg, and U) incorporated in coral skeletons are widely used as robust paleothermometers. The ratios of strontium/calcium (Sr/Ca), magnesium/calcium (Mg/Ca), and uranium/calcium (U/Ca) are largely determined by the temperature-dependent distribution coefficient of Sr/Ca, Mg/Ca, and U/Ca between aragonite and seawater. When sea surface temperature increases, the Sr/Ca and U/Ca ratios of the coral skeleton decrease while Mg/Ca ratio increases.

Since the pioneering work by Smith et al., (1979) and Beck et al., (1992), the Sr/Ca ratio of coral skeleton is the most extensively used proxy for reconstructing past SSTs. A large number of successful climate reconstructions using coral Sr/Ca further prove that Sr/Ca ratio is an good sea surface temperature proxy (e.g., Beck et al., 1992; McCulloch et al., 1994; Alibert and McCulloch, 1997; Gagan et al., 1998; Hughen et al., 1999; Swart et al., 2002; Winter et al., 2003; Cohen and Hart, 2004; Corrège et al., 2004; Felis et al., 2004; Pfeiffer et al., 2006; Goodkin et al., 2008b; Abram et al., 2009; Asami et al., 2009; Felis et al., 2009; Felis et al., 2010; Hetzinger et al., 2010).

No	Study	Location	b	a	Species
1	Mitsuguchi et al. (1996)	Ishigaki island, ECS – Pacific	10.543	-0.0608	*Porites lutea*
2	Shen et al. (1996)	Taiwan, SCS	10.307	-0.0505	*Porites lutea*
3	Wei et al. (2000)	Hainan island, SCS	10.600	-0.0504	*Porites lutea*
4	Yu et al. (2005)	Leizhou Peninsula, SCS	9.836	-0.0424	*Porites lutea*
5	Sun et al. (2005)	Xisha island, ESVN	10.327	-0.0534	*Porites sp.*
6	Mitsuguchi et al. (2008)	Con Dao island, ESVN	10.105	-0.0446	*Porites sp.*
7	A. Bolton et al. (2014)	Hon Tre island, ESVN	10.573	-0.055	*Porites sp.*
8	Gagan (1998)	Pacific, Australia	10.78	-0.066	*Porites lutea*

9	Marshall and McCulloch (2002)	Pacific, Australia	10.4	-0.0575	*Porites lutea*
10	Linsley et al. (2004)	Pacific, Fiji	10.65	-0.053	*Porites lutea*
11	Felis et al. (2009)	Pacific NW, Ogasawara	10.781	-0.0597	*Porites sp.*
12	Corrège (2006)	Pacific, N. Caledonia	10.407	-0.0576	*Porites sp.*
13	Zinke et al. (2004)	Madagascar	10.323	-0.05	*Porites lobata*

Table 1.2. *Table of published Sr/Ca-SST relationships for near-monthly sampling resolution expressed in the form of Sr/Ca (mmol/mol) = a x SST (°C) + b, where a is the slope and b the intercept.*

When ambient sea surface temperature increases, corals incorporate less Sr into their calcium carbonate and thus, record the SST of the ambient sea water as they grow (Smith et al., 1979; Beck et al., 1992). Recent analytical improvements in the application of Sr/Ca paleothermometry combined with the development of a new high-precision method of Sr/Ca determination, via Inductively Coupled Plasma Atomic Emission Spectrophotometer (ICP-AES) that compares very regularly coral samples values to a reference solution (Schrag, 1999).

During the aragonite skeleton formation of coral, both Sr and Ca are incorporated into the skeletal structures. Sr2+ mainly replaces to Ca2+ in crystal lattice (Kinsman and Holland, 1969). Because of the chemistry of Sr2+ is very similar to Ca2+, sothat their behaviour is similar. The Sr/Ca ratio in coral is believed to be predominantly controlled by two factors, (1) the Sr/Ca activity ratio of seawater and (2) the Sr/Ca distribution coefficient (D_{Sr}) between aragonite and seawater (Smith et al., 1979). Therefore, when Sr is picked up from a well defined solution, the Sr/Ca concentration in coral can be calculated by its distribution coefficient:

$$D_{Sr} = (Sr/Ca)_{coral}/(Sr/Ca)_{seawater}$$

Although Sr and Ca are very conservative elements in seawater, the seawater Sr/Ca ratio is effected by weathering of exposed aragonite on the continental shelves during low-sea level stand (Stoll and Schrag, 1998). Moreover, small changes in coral skeleton Sr/Ca concentration have been recorded due to coral symbionts, biological activities (called as “vital effects”, as well as other local effects (de Villiers et al., 1994; de Villiers et al., 1995; Shen et al., 1996; de Villiers, 1999; Cohen et al., 2002).

Despite the potential of coral Sr/Ca paleothermometry, there are several notable concerns that have prevented the acceptance and validity of coral Sr/Ca as a robust paleothermometer: 1) each species modern coral calibrated to instrumental SST shows a different coral Sr/Ca-SST relationship in both slope and intercept and 2) coral-based SST reconstructions in the tropical ocean for the Last Glacial Maximum (LGM) have shown SST conditions 2 to 4 times cooler than recorded by other marine paleoproxies (Beck et al., 1992), both implying that the Sr/Ca ratio in coral skeleton is not a simple a thermodynamic relationship (Marshall and McCulloch, 2002).

These all demonstrate that the coral Sr/Ca ratio is a good proxy of the past SST and therefore, judicious strategies should be used to extract robust estimations of the coral Sr/Ca-derived SST variability.

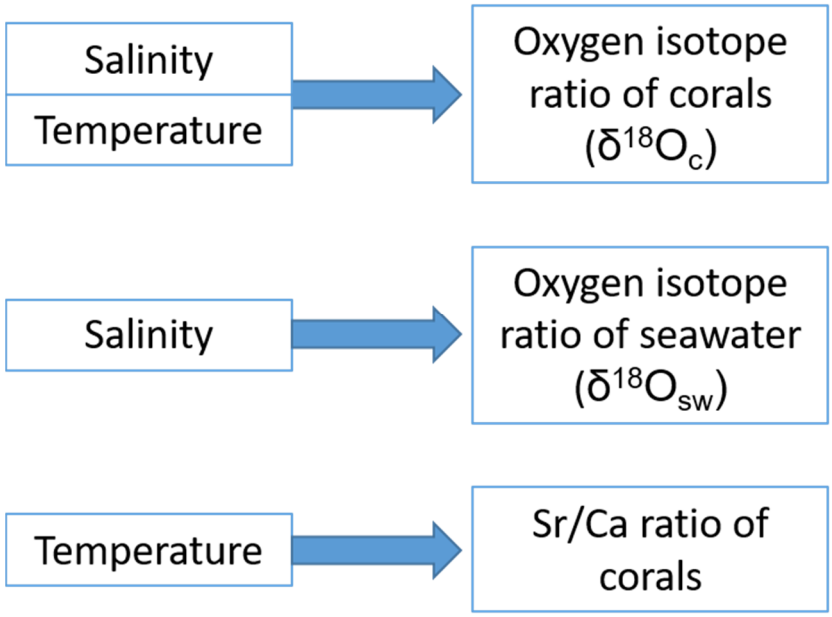

Figure 1.4. Sea surface condition parameters influence on geochemical record in coral

2.2. Coral $\delta^{18}O$, a combined temperature and salinity proxy

The $\delta^{18}O$ of coral skeleton is influenced by both sea surface temperature and oxygen isotopic composition of ambient seawater ($\delta^{18}Osw$). The $\delta^{18}Osw$ is linearly related to the sea surface salinity (SSS). $\delta^{18}Osw$ is consistent to paleoclimatology because it is closely related to the balance between precipitation and evaporation, and therefore $\delta^{18}Osw$ reconstruction could expose important information about past changes in hydrological cycle. However, because the $\delta^{18}O$ of coral skeletons is a function of both SST and $\delta^{18}Osw$ (Weber and Woodhead, 1972), it is it is normally difficult to devide the effects of SST and $\delta^{18}Osw$ by using coral $\delta^{18}O$ only. Therefore, in association with the coral Sr/Ca-based SST reconstruction, coral $\delta^{18}O$ can be used to reconstruct $\delta^{18}Osw$, a critical oceanographic parameter. Several studies have used paired coral Sr/Ca and $\delta^{18}Oc$ in order to appreciate past changes in the hydrological cycle recorded in the coral skeletons (McCulloch et al., 1994; Gagan et al., 1998; Ren et al., 2003; Zinke et al., 2004; Sun et al., 2005; Linsley et al., 2006; Pfeiffer et al., 2006; Cahyarini et al., 2008; Felis et al., 2009; Hetzinger et al., 2010).

Basically, $\delta^{18}O$ is a measure of the ratio between heavy and light oxygen isotopes ^{18}O and ^{16}O, respectively, in reference to a standard. This oxygen isotope ratio is reported in part per thousand or "per mil" (‰) and is calculated as follows:

$$\delta^{18}O = (((^{18}O/^{16}O)sample/(^{18}O/^{16}O)standard)-1)*1000$$

where the standard has a known isotopic composition such as Pee Dee Belemnite (PDB).

Pioneer studies by McCulloch et al., (1994) and Gagan et al., (1998; 2000) attempted to quantitatively separate the effects of SST from those of δ^{18}Osw on coral skeletal δ^{18}O, by using paired coral δ^{18}O and Sr/Ca analysis on the same coral samples. The authors estimated the relationship of coral δ^{18}O and SST, as well as Sr/Ca and SST, using univariate linear regression equations. These equations are then used to convert both proxies to temperature, in order to subtract the temperature component from coral δ^{18}O as described below:

$$\delta^{18}O_{coral} = \delta^{18}O_{SST} + \delta^{18}O_{sw}$$

Where

$$\delta^{18}O_{SST} = \gamma 1/\beta 1\ (Sr/Ca_{coral})$$

therefore,

$$\delta^{18}O_{sw} = \delta^{18}O_{coral} - \gamma 1/\ \beta 1\ (Sr/Ca_{coral})$$

where $\delta^{18}O_{SST}$ and δ^{18}Osw are the temperature and seawater oxygen isotopic component of the measured δ^{18}Ocoral, respectively. Here, $\gamma 1$ and $\beta 1$ are the δ^{18}O-SST and Sr/Ca-SST regression slopes, respectively.

The oxygen isotopic composition of sea water (δ^{18}Osw) and SSS covary in the surface ocean waters on a global scale (Schmidt et al., 1999 "Global Seawater Oxygen-18 Database - v1.20" http://data.giss.nasa.gov/o18 data/). The positive relationship between the δ^{18}Osw and SSS is a critical relationship in paleoclimatology, because in combination with thermodynamic properties of the ambient sea water it provides the chance to estimate the density of sea water, an important oceanographic parameters involved in the meridional overturning circulation in the North Atlantic. Both parameters are largely related to the hydrological cycle, with higher SSS and δ^{18}Osw values observed in regions where evaporation exceeds precipitation, whereas lower values are characteristic of regions dominated by precipitation and river runoff. Furthermore, both parameters of the surface waters are influenced by oceanic advection and diffusion processes. Since the relationship between SSS and δ^{18}Osw has been extensively studied in past few decades (Schmidt, 1999; Delaygue et al., 2000), a unique study performed on Caribbean seawater (Watanabe et al., 2001) yielded to the conclusion that seasonal variation of δ^{18}Osw is mostly governed by SSS changes. The δ^{18}Osw-SSS relationship from these data is:

$$\delta^{18}\text{Osw} = 0.204\ (\pm 0.03)*\text{SSS} - 6.54\ (\pm 0.68)\ (r = 0.93,\ n = 20)$$

Consequently, reconstruction of past changes in Caribbean SSS on time scales ranging from seasonal to multidecadal can be achieved from the reconstructed δ^{18}Osw inferred from the paired coral Sr/Ca and δ^{18}O measurements. Such an approach performed on tropical Atlantic corals will provide unique insights on the variations of hydrological cycle in the southern Caribbean Sea on these time scales.

2.3. Ba/Ca variation

Barium (Ba) has a nutrient-like distribution in the ocean, generally depleting in surface waters and enriching in deep waters, and such concentration profiles indicate involvement in

biological processes (Lea and Boyle, 1989; Dymond and Collier, 1996; Stecher and Kogut, 1999; Paytan and Griffith, 2007). The concentrations of Ba in seawater (Sternberg et al., 2008) and sediment (Pfeifer et al., 2001; Paytan and Griffith, 2007) have been recently employed as proxies for past biogeochemical processes. Ba incorporated into bivalve shells has been used as a tracer of local primary productivity (Vander et al., 2000; Elliot et al., 2009).

In scleractinian corals, Ba can substitute for Ca into the crystal lattice of coral aragonite (Lea et al., 1989; Fallon et al., 1999; Sinclair and McCulloch, 2004), with a partition coefficient $D_{Ba} = Ba/Ca_{coral}/Ba/Ca_{seawater} \approx 1$) (Lea et al., 1989; Alibert et al., 2003). Its skeletal concentration faithfully records the concentration of Ba in the ambient ocean, thus making it a potential tracer of a number of different oceanographic processes. Coral Ba/Ca, first studied by Bowen (1956) and Harriss and Almy (1964), is thought to reflect ambient seawater conditions, and therefore parallels the environment in which the coral grew. Coralline Ba/Ca has been shown to track upwelling and/or coastal runoff, depending upon the local sources of barium to surface waters (e.g. Lea et al., 1989; Sinclair and McCulloch, 2004b; Sinclair, 2005; Montaggioni et al., 2006; Fleitmann et al., 2007; Prouty et al., 2010; Maina et al., 2012; Moyer et al., 2012). Barium is removed from the dissolved phase in the upper water column by the precipitation of micron-scale barite crystals, formed in microenvironments of decaying organic matter and probably by other poorly described mechanisms as well (Dehairs et al., 1980; Bishop, 1988; Ganeshram et al., 2003). Barium is then returned to the dissolved phase in the thermocline and below, such that the resultant vertical concentration profile resembles that of silicate, which is remineralized deeper than nitrate and phosphate. Because of this ‘‘nutrient- like” Ba_{sw} water column profile, Ba/Ca in surface corals has been used to reconstruct changes in the upwelling of nutrient-rich thermocline waters (Lea et al., 1989; Fallon et al., 1999; Montaggioni et al., 2006; Allison and Finch, 2007). However, the increase of Ba_{sw} with depth is relatively subtle compared to the major nutrients nitrate and phosphate. Therefore, terrestrial runoff inputs of Ba to coastal upwelling sites can compromise the interpretation of Ba/Ca as an upwelling proxy in some locations. In coastal regions affected by river discharge, skeletal Ba/Ca has been shown to record changes in sediment discharge, as barium desorbs from suspended sediment in low salinity estuarine waters, increasing Ba_{sw} and thus, skeletal Ba/Ca coral (Alibert et al., 2003; McCulloch et al., 2003; Sinclair and McCulloch, 2004a; Prouty et al., 2008, 2010; Carriquiry and Horta-Puga, 2010; Horta-Puga and Carriquiry, 2012; Maina et al., 2012; Moyer et al., 2012; Mallela et al., 2013).

Moreover, inshore coral skeletal Ba/Ca records correlate well with flood events (or freshwater events) associated with intense rainfall during wet seasons allowing monitoring of long term changes in rainfall patterns. Ba/Ca peaks match well with peaks in skeletal fluorescence, a robust proxy for freshwater flood events (Isdale, 1984; Lough et al., 2002), confirming that the Ba is sourced mainly from river discharge (Sinclair and McCulloch, 2004).

4. Aim of this study

The reasons to choose this research:

- In recent years, paleoclimate, climate change and its effects on marine environments are one of great concern of the World in general and Viet Nam Government in particular. In Viet Nam, researches using coral geochemical records for reconstruction of paleoclimate and paleoenvironment are relatively limited. Therefore, this research will be very important.

- Mekong river and Mekong Delta have an important role to economic of Viet Nam. This study will contribute to prevent the disaster due to floods from Mekong River and climate changes, and to promote economic development in the Mekong Delta.

- Coral reefs in Vietnam are very rich and diverse with many different species. This will be good conditions to carry out this study.

- The VNU University of Science has invested in modern equipment and laboratories for paleoclimate and climate change researches. This will be a new direction for researching and education at our university.

The aim of this study is to examine the potential of geochemical records from Porites coral in Con Dao island as proxies for climate changes, environment and East Asian monsoon variability. Using the correlation between them to reconstruct SST, SSS, Mekong river discharge and indicate flood events from Mekong delta. Establish the relationship between geochemical of corals with some phenomenon such as: El nino, La lina…

REFERENCES

1. Bradley, R. S., 1999: Paleoclimatology: reconstructing climates of the Quaternary (Vol. 68), 132, 247. Academic Press.
2. Hoegh-Guldberg, O., 1999: Climate change, coral bleching and the future of the world's coral reefs. Marine and freshwater research 50(8), 839–66.
3. Lough, J. M., & Barnes, D. J., 1997: Several centuries of variation in skeletal extension, density and calcification in massive Porites colonies from the Great Barrier Reef: A proxy for seawater temperature and a background of variability against which to identify unnatural change. Journal of Experimental Marine Biology and Ecology 211(1), 29-67.
4. Spalding, M., Ravilious, C., & Green, E. P., 2001: World atlas of coral reefs. Univ of California Press.
5. Veron, J. E. N., 2000: Corals of the World. Australian Institute of Marine Science, 3 vol.
6.
7. Abram, N.J., McGregor, H.V., Gagan, M.K., Hantoro, W.S. and Suwargadi, B.W., 2009. Oscillations in the southern extent of the Indo-Pacific Warm Pool during the mid-Holocene. Quaternary Science Reviews 28, 2794-2803.
8. Alibert C, Kinsley L, Fallon S J, McCulloch M T, Berkelmans R, McAllister F, 2003. Source of trace element variability in Great Barrier Reef corals affected by the Burdekin flood plumes. Geochimica et Cosmochimica Acta, 67(2): 231–246.

9. Alibert C., Kinsley L., Fallon S., McCulloch M., Berkelmans R. and McAllister F. (2003) Source of trace element variability in Great Barrier Reef corals affected by the Burdekin flood plumes. Geochim. Cosmochim. Acta 67, 231–246.
10. Alibert, C. and McCulloch, M.T., 1997. Strontium/Calcium Ratios in Modern Porites Corals From the Great Barrier Reef as a Proxy for Sea Surface Temperature: Calibration of the Thermometer and Monitoring of ENSO. Paleoceanography, 12(3), 345-363.
11. Allison N. and Finch A. A. (2007) High temporal resolution Mg/ Ca and Ba/Ca records in modern Porites lobata corals. Geochem. Geophys. Geosyst. 8, Q05001.
12. Allison, N. and Finch, A.A., 2004. High-resolution Sr/Ca records in modern Porites lobata corals: Effects of skeletal extension rate and architecture. Geochemistry Geophysics Geosystems 5, Q05001, doi:10.1029/2004GC000696.
13. Asami, R., Felis, T., Deschamps, P., Hanawa, K., Iryu, Y., Bard, E., Durand, N. and Murayama, M., 2009. Evidence for tropical South Pacific climate change during the Younger Dryas and the Bølling-Allerød from geochemical records of fossil Tahiti corals. Earth and Planetary Science Letters 288, 96-107.
14. Bard, E., Hamelin, B., Fairbanks, R.G., Zindler, A., 1990: Calibration of the 14C timescale over the past 130,000 years using mass spectrometric U –Th ages from Barbados corals. Nature 345, 405 – 410.
15. Beck, J.W., Edwards, R.L., Ito, E., Taylor, F.W., Recy, J., Rougerie, F., Joannot, P. and Henin, C., 1992. Sea-Surface Temperature from Coral Skeletal Strontium/Calcium Ratios. Science 257, 644-647.
16. Bishop J. K. B. (1988) The barite-opal-organic carbon association in oceanic particulate matter. Nature 332, 341–343.
17. Bowen, H.J.M., 1956. Strontium and barium in sea water and marine organisms. J. Mar. Biol. Assoc. UK 35:451–460. http://dx.doi.org/10.1017/S0025315400010298
18. Cahyarini, S.Y., Pfeiffer, M., Timm, O., Dullo, W.-C. and Schönberg, D.G., 2008. Reconstructing seawater d18O from paired coral d18O and Sr/Ca ratios: Methods, error analysis and problems, with examples from Tahiti (French Polynesia) and Timor (Indonesia). Geochimica et Cosmochimica Acta 72, 2841-2853.
19. Carriquiry J. D. and Horta-Puga G. (2010) The Ba/Ca record of corals from the Southern Gulf of Mexico: contributions from land-use changes, fluvial discharge and oil-drilling muds. Mar. Pollut. Bull. 60, 1625–1630
20. Carriquiry, J., Risk, M. J., & Schwarcz, H. P., 1994: Stable isotope geochemistry of corals from Costa Rica as proxy indicator of the El Niño/ Southern Oscillation (ENSO). Geochimica et Cosmochimica Acta 58(1), 335-351.
21. Chu, T.H., Guttnam, H., Droogers, P. and Aerts, J. (2003). Water, climate, food and environment in the Mekong basin in Southeast Asia – Final report. International Water Management Institute, Mekong River Commission Secretariat, Institute of Environmental Studies.

22. Cohen, A.L. and Hart, S.R., 2004. Deglacial sea surface temperatures of the western tropical Pacific: A new look at old coral. Paleoceanography 19.
23. Cohen, A.L., Owens, K.E., Layne, G.D. and Shimizu, N., 2002. The Effect of Algal Symbionts on the Accuracy of Sr/Ca Paleotemperatures from Coral. Science 296, 331-333.
24. Corrège, T., 2006: Sea surface temperature and salinity reconstruction from coral geochemical tracers. Paleogeography, Paleoclimatology, Paleoecology 232, 408-428.
25. Corrège, T., Gagan, M.K., Beck, J.W., Burr, G.S., Cabioch, G. and Le Cornec, F., 2004. Interdecadal variation in the extent of South Pacific tropical waters during the Younger Dryas event. Nature 428, 927-929.
26. de Villiers, S., 1999. Seawater strontium and Sr/Ca variability in the Atlantic and Pacific oceans. Earth and Planetary Science Letters 171, 623-634.
27. de Villiers, S., Nelson, B.K. and Chivas, A.R., 1995. Biological Controls on Coral Sr/Ca and 18O Reconstructions of Sea Surface Temperatures. Science 269, 1247-1249.
28. de Villiers, S., Shen, G.T. and Nelson, B.K., 1994. The Sr/Ca-temperature relationship in coralline aragonite: Influence of variability in (Sr/Ca)seawater and skeletal growth parameters.
29. Dehairs F., Chesselet R. and Jedwab J. (1980) Discrete suspended particles of barite and the barium cycle in the open ocean. Earth Planet. Sci. Lett. 49, 528–550.
30. Delaygue, G., Jouzel, J. and Dutay, J.-C., 2000. Oxygen 18-salinity relationship simulated by anoceanic general circulation model. Earth and Planetary Science Letters 178, 113-123.
31. Dymond J, Collier R, 1996. Particulate barium fluxes and their relationships to biological productivity. Deep Sea Research Part II: Topical Studies in Oceanography, 43(4-6): 1283–1308.
32. Elliot M, Welsh K, Chilcott C, McCulloch M, Chappell J, Ayling B, 2009. Profiles of trace elements and stable derived from giant long-lived Tridacna gigas bivalves: Potential applications in paleoclimate studies. Palaeography, Palaeoclimatology, Palaeoecology, 280(1-2): 132–142.
33. Fallon S J, McCullochM T, vanWoesik R, Sinclair D J, 1999. Corals at their latitudinal limits: laser ablation trace element systematics in Porites from Shirigai Bay, Japan. Earth and Planetary Science Letters, 172(3- 4): 221–238.
34. Felis, T., Lohmann, G., Kuhnert, H., Lorenz, S.J., Scholz, D., Patzold, J., Al-Rousan, S.A. and AlMoghrabi, S.M., 2004. Increased seasonality in Middle East temperatures during the last interglacial period. Nature 429, 164-168.
35. Felis, T., Suzuki, A., Kuhnert, H., Rimbu, N. and Kawahata, H., 2010. Pacific Decadal Oscillation documented in a coral record of North Pacific winter temperature since 1873. Geophys. Res. Lett. 37, L14605.
36. Gagan, M.K., Ayliffe, L.K., Hopley, D., Cali, J.A., Mortimer, G.E., Chappell, J., McCulloch, M.T. and Head, M.J., 1998. Temperature and Surface-Ocean Water Balance of the Mid-Holocene Tropical Western Pacific. Science 279, 1014-1018.

37. Gagan, M.K., Ayliffe, L.K., Hopley, D., Cali, J.A., Mortimer, G.E., Chappell, J., McCulloch, M.T. and Head, M.J., 1998. Temperature and Surface-Ocean Water Balance of the Mid-Holocene Tropical Western Pacific. Science 279, 1014-1018.
38. Ganeshram R. S., Franc¸ois R., Commeau J. and Brown-Leger S. L. (2003) An experimental investigation of barite formation in seawater. Geochim. Cosmochim. Acta 67, 2599–2605.
39. Geochimica et Cosmochimica Acta 58, 197-208.
40. Goodkin, N.F., Hughen, K.A., Doney, S.C. and Curry, W.B., 2008b. Increased multidecadal variability of the North Atlantic Oscillation since 1781. Nature Geoscience 1, 844-848
41. Grottoli, A. G. (2001). Past climate from corals. Encyclopedia of Ocean Sciences (Second Edition), 338-347. Academic Press.
42. Grottoli, A. G., & Eakin, C. M., 2007: A review of modern coral δ18O and Δ14C proxy records. Earth-Science Reviews 81(1), 67-91.
43. Harriss, R.C., Almy Jr., C.C., 1964. A preliminary investigation into the incorporation and distribution of minor elements in the skeletal material of Scleractinian corals. Bull. Mar. Sci. 14, 418–422.
44. Hetzinger, S., Pfeiffer, M., Dullo, W.-C., Garbe-Schönberg, D. and Halfar, J., 2010. Rapid 20th century warming in the Caribbean and impact of remote forcing on climate in the northern tropical Atlantic as recorded in a Guadeloupe coral. Palaeogeography, Palaeoclimatology, Palaeoecology 296, 111-124.
45. Horta-Puga G. and Carriquiry J. D. (2012) Coral Ba/Ca molar ratios as a proxy of precipitation in the northern Yucatan Peninsula, Mexico. Appl. Geochem. 27, 1579–1586.
46. Hughen, K.A., Schrag, D.P., Jacobsen, S.B. and Hantoro, W., 1999. El Niño during the Last Interglacial Period recorded by a fossil coral from Indonesia. Geophys. Res. Lett. 26, 3129-3132.
47. Isdale, P., 1984. Fluorescent bands in massive corals record centuries of coastal rainfall. Nature 310 (5978), 578–579.
48. Juillet-Leclerc, A., Reynaud, S., Rollion-Bard, C., Cuif, J.P., Dauphin, Y., Blamart, D., FerrierPagès, C. and Allemand, D., 2009. Oxygen isotopic signature of the skeletal microstructures in cultured corals: Identification of vital effects. Geochimica et Cosmochimica Acta 73, 5320-5332.
49. Kinsman, D.J.J. and Holland, H.D., 1969. The co-precipitation of cations with CaCO3--IV. The coprecipitation of Sr2+ with aragonite between 16° and 96°C. Geochimica et Cosmochimica Acta 33, 1-17.
50. Lea D. W, Shen G. T, Boyle E. A, 1989. Coralline barium records temporal variability in equatorial Pacific upwelling. Nature, 340: 373–376.
51. Linsley, B.K., Kaplan, A., Gouriou, Y., Salinger, J., deMenocal, P.B., Wellington, G.M. and Howe, S.S., 2006. Tracking the extent of the South Pacific Convergence Zone since the early 1600s. Geochemistry Geophysics Geosystems 7, Q05003, doi:10.1029/2005GC001115.
52. Lough, J.M., 2004. A strategy to improve the contribution of coral data to high-resolution paleoclimatology. Palaeogeography, Palaeoclimatology, Palaeoecology 204, 115-143.

53. Maina J., de Moel H., Vermaat J. E., Bruggemann J. H., Guillaume M. M., Grove C. A., Madin J. S., Mertz-Kraus R. and Zinke J. (2012) Linking coral river runoff proxies with climate variability, hydrology and land-use in Madagascar catchments. Mar. Pollut. Bull. 64, 2047–2059.
54. Mallela J., Lewis S. E. and Croke B. (2013) Coral skeletons provide historical evidence of phosphorus runoff on the Great Barrier reef. PLoS ONE 8, e75663.
55. Marshall, J.F. and McCulloch, M.T., 2002. An assessment of the Sr/Ca ratio in shallow water hermatypic corals as a proxy for sea surface temperature. Geochimica et Cosmochimica Acta 66, 3263-3280.
56. McCulloch M., Fallon S., Wyndham T., Hendy E., Lough J. and Barnes D. (2003) Coral record of increased sediment flux to the inner Great Barrier Reef since European settlement. Nature 421, 727–730.
57. McCulloch, M.T., Gagan, M.K., Mortimer, G.E., Chivas, A.R. and Isdale, P.J., 1994. A highresolution Sr/Ca and 18O coral record from the Great Barrier Reef, Australia, and the 1982- 1983 El Niño. Geochimica et Cosmochimica Acta 58, 2747-2754.
58. McCulloch, M.T., Gagan, M.K., Mortimer, G.E., Chivas, A.R. and Isdale, P.J., 1994. A highresolution Sr/Ca and 18O coral record from the Great Barrier Reef, Australia, and the 1982-1983 El Niño. Geochimica et Cosmochimica Acta 58, 2747-2754.
59. Montaggioni L. F., Le Cornec F., Corre `ge T. and Cabioch G. (2006) Coral barium/calcium record of mid-Holocene upwelling activity in New Caledonia, South-West Pacific. Palaeogeogr. Palaeoclimatol. Palaeoecol. 237, 436–455.
60. Moyer R. P., Grottoli A. G. and Olesik J. W. (2012) A multiproxy record of terrestrial inputs to the coastal ocean using minor and trace elements (Ba/Ca, Mn/Ca, Y/Ca) and carbon isotopes (d13C, D14C) in a nearshore coral from Puerto Rico. Paleo- ceanography 27, PA3205.
61. MRC (2003). State of the Basin report. The Mekong River Commission, Phnom Penh, Cambodia.
62. Paytan A, Griffith E M, 2007. Marine barite: Recorder of variations in ocean export productivity. Deep-Sea Research II, 54(5-7): 687–705.
63. Pfeifer K, Kasten S, Hensen C, Schulz H D, 2001. Reconstruction of primary productivity from the barium contents in surface sediments of the South Atlantic Ocean. Marine Geology, 177(1-2): 13–24.
64. Pfeiffer, M., Timm, O., Dullo, W.-C. and Garbe-Schönberg, D., 2006. Paired coral Sr/Ca and d18O records from the Chagos Archipelago: Late twentieth century warming affects rainfall variability in the tropical Indian Ocean. Geology 34, 1069-1072.
65. Philander, S.G., 1990: El Niño, La Niña and the Southern Oscillation. Academic Press, New York.
66. Prouty N. G., Field M. E., Stock J. D., Jupiter S. D. and McCulloch M. (2010) Coral Ba/Ca records of sediment input to the fringing reef of the southshore of Moloka'i, Hawai'i over the last several decades. Mar. Pollut. Bull. 60, 1822–1835.

67. Prouty N. G., Hughen K. A. and Carilli J. (2008) Geochemical signature of land-based activities in Caribbean coral surface samples. Coral Reefs 27, 727–742.
68. Ren, L., Linsley, B.K., Wellington, G.M., Schrag, D.P. and Hoegh-guldberg, O., 2003. Deconvolving the 18O seawater component from subseasonal coral 18O and Sr/Ca at Rarotonga in the southwestern subtropical Pacific for the period 1726 to 1997. Geochimica et Cosmochimica Acta 67, 1609-1621.
69. Schmidt, G.A., 1999. Forward Modeling of Carbonate Proxy Data from Planktonic Foraminifera Using Oxygen Isotope Tracers in a Global Ocean Model. Paleoceanography 14, 482-497.
70. Schrag, D.P., 1999. Rapid Analysis of High-Precision Sr/Ca Ratios in Corals and Other Marine Carbonates. Paleoceanography 14, 97-102.
71. Shen, C.-C., Lee, T., Chen, C.-Y., Wang, C.-H., Dai, C.-F. and Li, L.-A., 1996. The calibration of D[Sr/Ca]versus sea surface temperature relationship for Porites corals. Geochimica et Cosmochimica Acta 60, 3849-3858.
72. Sinclair D J, McCulloch M T, 2004. Corals record low mobile barium concentrations in the Burdekin River during the 1974 flood: evidence for limited Ba supply to rivers? Palaeogeography, Palaeoclimatology, Palaeoecology, 214(1-2): 155–174.
73. Sinclair D. J. (2005) Non-river flood barium signals in the skeletons of corals from coastal Queensland, Australia. Earth Planet. Sci. Lett. 237, 354-369.
74. Smith, S.V., Buddemeier, R.W., Redalje, R.C. and Houck, J.E., 1979. Strontium-Calcium Thermometry in Coral Skeletons. Science 204, 404-407.
75. Sternberg E, Jeandel C, Robin E, Souhaut M, 2008. Seasonal cycle of suspend- ed barite in the mediterranean sea. Geochimica et Cosmochimica Acta, 72(16): 4020–4034.
76. Stoll, H.M. and Schrag, D.P., 1998. Effects of Quaternary Sea Level Cycles on Strontium in Seawater. Geochimica et Cosmochimica Acta 62, 1107-1118.
77. Sun, D., Gagan, M.K., Cheng, H., Scott-Gagan, H., Dykoski, C.A., Edwards, R.L. and Su, R., 2005. Seasonal and interannual variability of the Mid-Holocene East Asian monsoon in coral [delta]18O records from the South China Sea. Earth and Planetary Science Letters 237, 69-84.
78. Swart, P.K., Elderfield, H. and Greaves, M.J., 2002. A high-resolution calibration of Sr/Ca thermometry using the Caribbean coral Montastraea annularis. Geochemistry Geophysics Geosystems 3, 8402, doi:10.1029/2002GC000306.
79. Vander P E, Dehairs F, Keppens E, Baeyens W, 2000. High resolution distribution of trace elements in the calcite shell layer of modern Mytilus edulis: Environmental and biological controls. Geochimica et Cosmochimica Acta, 64(6): 997–1011.
80. Watanabe, T., Winter, A. and Oba, T., 2001. Seasonal changes in sea surface temperature and salinity during the Little Ice Age in the Caribbean Sea deduced from Mg/Ca and 18O/16O
81. Weber, J.N. and Woodhead, P.M.J., 1972. Temperature dependence of oxygen-18 concentration in reef coral carbonates. Journal of Geophysical Research vol. 77, 463.

82. Winter, A., Paul, A., Nyberg, J., Oba, T., Lundberg, J., Schrag, D. and Taggart, B., 2003. Orbital control of low-latitude seasonality during the Eemian. Geophysical Research Letters 30, 1163, doi:10.1029/2002GL016275.
83. Zinke, J., Dullo, W.C., Heiss, G.A. and Eisenhauer, A., 2004. ENSO and Indian Ocean subtropical dipole variability is recorded in a coral record off southwest Madagascar for the period 1659 to 1995. Earth and Planetary Science Letters 228, 177-194.

Chapter 2
MATERIALS AND METHODS

1. Sampling site and climate data

Con Dao island is located at 8°41′35″N 106°34′36″E, in the south-east region of Viet Nam. The distance from Con Dao islands to Me Kong river mouth is about 90 km (Figure 2.1). It sits in the Asian monsoon climate and influenced by ocean climate. By dint of this, Con Dao weather is portrayed by characteristics of sub-equatorial and ocean climate. In a year, there are two monsoon movements: south-west monsoon from May to September, and north-east monsoon from October to April correspond to East Asian summer monsoon and East Asian winter monsoon, respectively. The climate of Con Dao island is characterized by two seasons: warm/wet season (from May to November) and cool/dry season (from December to April).

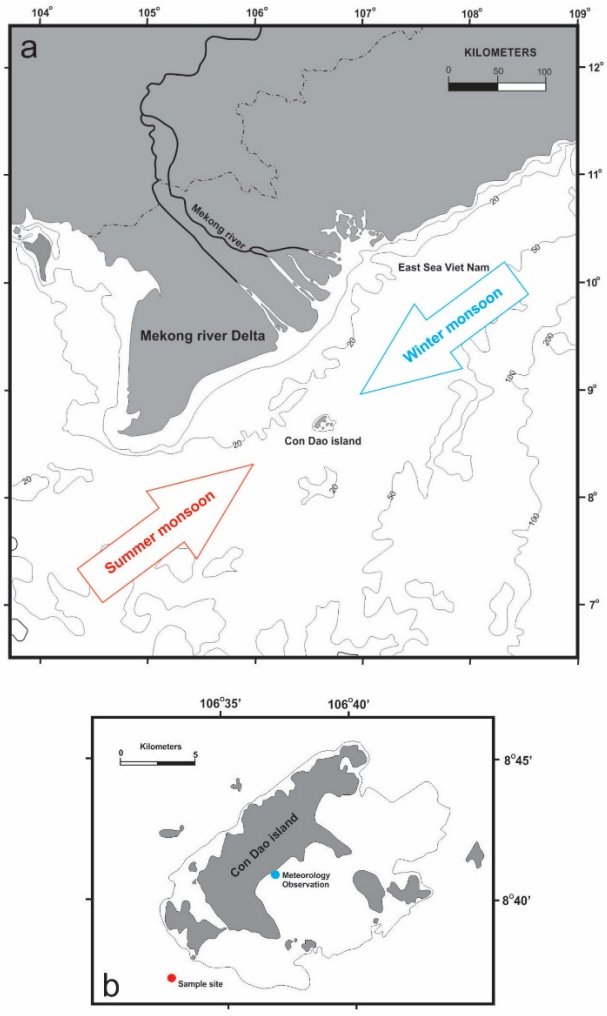

Figure 2.1. (a) Location of the East Sea and Mekong River of Vietnam. The climate of this area is strongly dominated by the East Asian monsoon: summer monsoon and winter monsoon correspond to southwesterly winds and northeasterly winds, respectively. Con Dao Island located in the ESVN, ~ 90 km from the mouth of the Mekong River. (b) Map of Con Dao Island showing the location of the sampling site at the southwest side of the island (red circle). Meteorological observation station (blue circle) located 15 km distance away from the sampling site.

The meteorological observation records (Figure 2.2) have been recorded since January 1980 in the Con Dao meteorological observation station (Institute of Hydrology and Meteorology of Vietnam), which is located in about 15 km away from the coral sampling site. The local mean sea surface temperature (SST) in Con Dao is 28.3^{O}C, within the range from 25^{O}C (monthly mean SST in January) to 31^{O}C (monthly mean SST in May). The annual precipitation is about 2,100 mm and 95% of this occurs in warm/wet season and reaches the highest in August to October. In contrast, precipitation is minimal in the cool (dry) season, when the North-east monsoon is active. The meteorological observation records show that the mean seasonal cycle of SSS is about 6‰ with a maximum of 34‰ in February – April and a minimum of 28‰ in October. The mean annual SSS is 32‰.

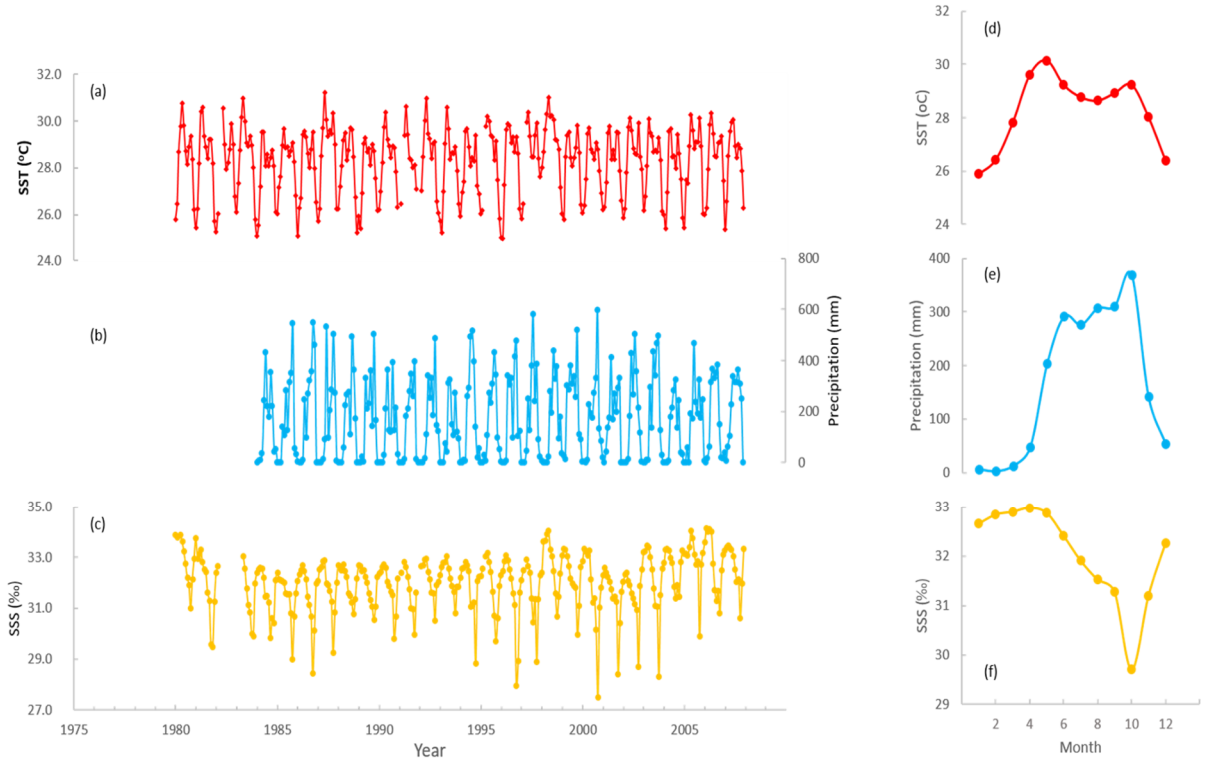

Figure 2.2. Monthly climate data recorded by meteorological observation station in Con Dao island (a) SST from 1980 to 2007, (b) Precipitation from 1984 to 2007, (c) SSS from 1980 to 2007 and calculated climatological data, respectively.

2. Sample preparation

In June 2006, we drilled 4 Porites sp. coral cores (CD-4) from water about 20 m depth in south-west side of Con Dao island (N 8^{o}33.43' E 106^{o}33'). The cores, taken vertically from the coral body, were 150 cm in total length and 5 cm in diameter.

The coral cores were cut into 5-mm-thick slabs using a diamond saw blade along the axis of major growth. Each coral slab was ultrasonically cleaned with deionized water for 10 min to remove surface contaminants. This procedure was repeated 3 times after which each coral piece was oven dried at 40 °C for 48 h. The slabs were then photographed under UV light and X-rayed. The UV photo and X-ray photo revealed luminescent banding and density banding in the coral,

respectively (Figure 2.3). There are 82 couple bands in total, and all bands are quite clear. The 82 couple bands were assumed to be annual growth bands covering the period AD 1922 – 2005.

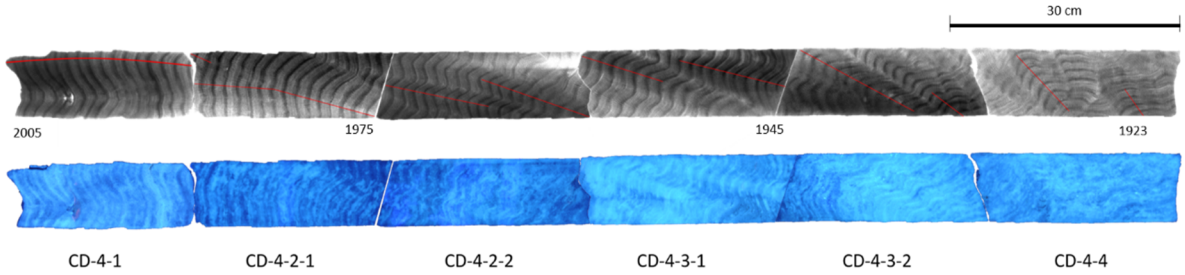

Figure 2.3. X-radiograph (top) and UV-luminescence photograph (bottom) of a coral skeletal core slab (Porites sp.) from Con Dao Island showing annual bands for AD 1922 - 2005. The UV photograph and X-ray photograph revealed clear luminescent banding and density banding in the coral, respectively. One year is represented by high-density/low-density couplet. The red lines indicate the measurement lines for geochemical analysis. The scale bars are 30 cm.

On the basis of the banding patterns in the UV-luminescence photo and X radiograph, 11 measurement lines were determined on the coral slabs for sampling along the skeletal growth direction. Along the measurement lines, 1050 sub-samples were drilled using a 0.8 mm diameter micro-drill at 1 mm intervals with a drilling depth of 1 mm.

3. Oxygen isotopes analysis

Coral stable isotope ratios were measured following the standard procedures on a Finnigan MAT 253 mass spectrometer with an automatic carbonate device (Kiel IV) in Hokkaido University (Figure 2.4). The coral powder was weighed, and 20-40 µg powder was reacted with 100% H_3PO_4 at 70^{O}C. Isotopic ratios are expressed in conventional delta notation in per mil units relative to Vienna Pee Dee belemnite through measurements of the isotopic ratio of CO_2 gas derived from National Bureau of Standards NBS-19 and NBS-18. The internal precision for $\delta^{18}O$ and $\delta^{13}C$ was ±0.04‰ and 0.08, respectively (n = 80).

Figure 2.4. The Finnigan MAT 253 mass spectrometer with an automatic carbonate device (Kiel IV) in Hokkaido University.

4. Trace elements analysis

Pretreatment of samples for trace elements analysis:

Because trace elements are highly effected by both to pre-existing surface contamination (detritus and organic) and contamination introduced in sample recovery and preparation. Therefore, chemical pretreatment steps in sample preparations for coral material are often necessary. I will test the analytical effects of chemical treatment on coral aragonite standard JCP1 and chose which methods can be used for my coral samples from Con Dao island.

Based on study of Watanabe et al., 2001, I use some of cleaning processes as follow:

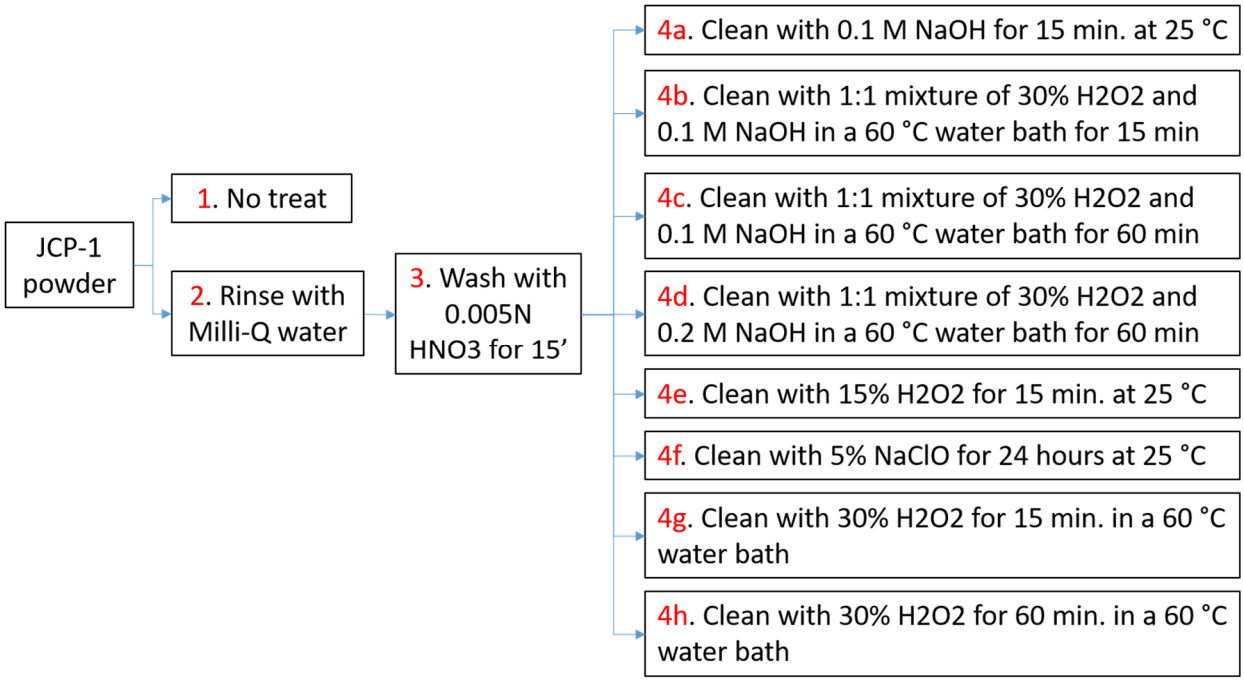

Figure 2.5. Some of cleaning processes use for testing in my research

Sr/Ca ratio in coral is relative stable and effect of organic compounds is negligible in aragonite corals (Amiel et al., 1973). Therefore I only chose the pretreatment method using for Ba/Ca and Mg/Ca analysis.

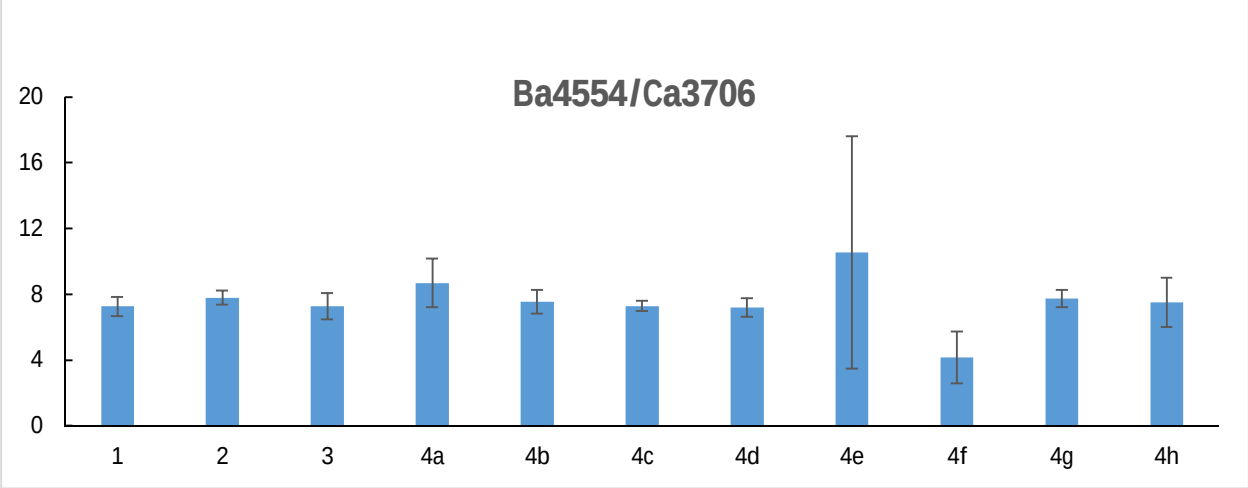

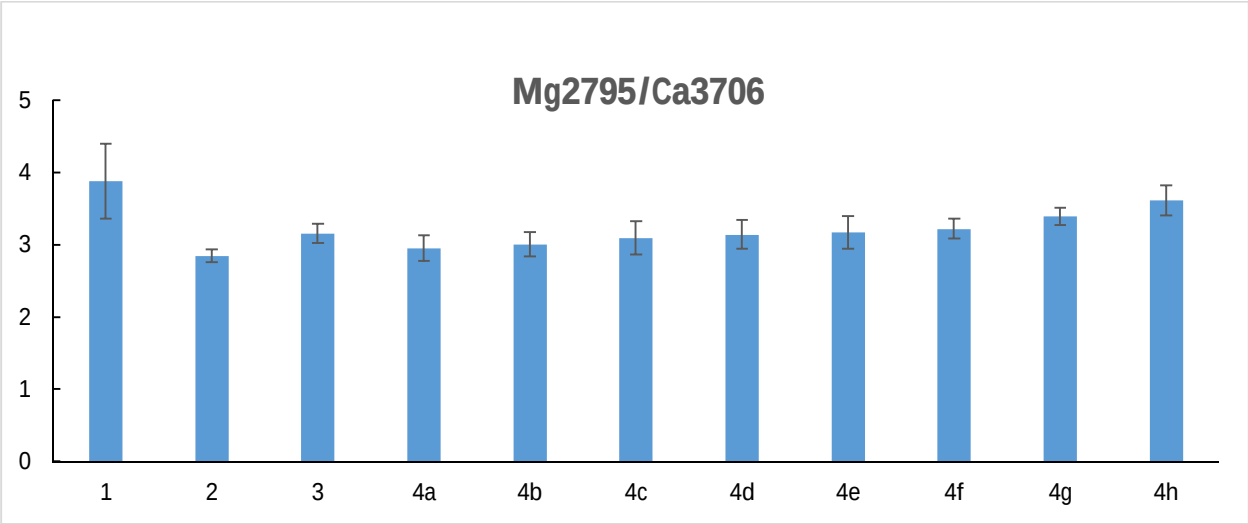

Figure 2.6. Ba/Ca and Mg/Ca result in JCP1 using for each cleaning processes. Error bar indicates standard deviation of results.

Each steps were measured 5 times, the result of Ba/Ca and Mg/Ca will be averaged values (Figure 2.6). My testing showed that Ba/Ca and Mg/Ca ratios in corals are significantly affected by chemical treatment. The standard deviation (2σ) of duplicate analysis were calcualted with each procedure. The highest and lowest standard deviation values of Ba/Ca ratios are 7.1 and 0.32 corresponding to organic clean 4e (with 5% NaClO for 24 hours at 25 °C) and 4c (with 1:1 mixture of 30% H_2O_2 and 0.1 M NaOH in a 60 °C water bath for 60 min), respectively. Standard deviation value of samples rinsed with milli-Q water is also noticeably, 0.44. The highest and lowest standard deviation values of Mg/Ca ratios are 0.51 and 0.089 corresponding to no pretreatment and rinse with milli-Q water, respectively. Due to Ba/Ca and Mg/Ca ratios will be calculated from 1 measument, therefore I should chose the procedure with best standard deviation for both. The step 2 (the sample washed with milli-Q water) show good standard deviation for both Ba/Ca and Mg/Ca. Therefore, I will apply this pretreatment method for my samples.

In order to measure the coral trace element ratio, we use inductively coupled plasma-atomic emission spectrometry (ICP-AES) in Hokkaido University. Sample solution for coral Sr/Ca ratios analysis was prepared by using 80-90 µg sample powder dissolved in 0.5 ml HNO_3 25% then add milli-Q to get a Ca concentration of 7 ppm.

Figure 2.7. The inductively coupled plasma-atomic emission spectrometry (ICP-AES) in Hokkaido University

For Mg/Ca and Ba/Ca ratios, the 115 – 128 µg powder sample was rinsed with 2 ml milli-Q water in ultrasonic bath for 10 minutes for removing the possible organic contamination. The solution was then centrifuged for 15 minutes and removed 1.8 ml milli-Q water. Residual solution was mixed with 0.5 ml HNO_3 25% and milli-Q to get a Ca concentration of 9 ppm. This analysis was held using ICP-AES, coupled to an ultrasonic nebulizer.

Accuracy was monitored by analyzing the Porites coral standard JCp-1. Analytical precision of the Sr/Ca, Mg/Ca and Ba/Ca determinations was 0.07%, 0.5 % and 1.2 % respectively.

5. Age model

We used the coral Sr/Ca ratios to create an age model for all proxies. Minima and maxima of the Sr/Ca ratios were tied to the maxima and minima of observed SST from Con Dao Island. The Sr/Ca data and instrumental SST were re-sampled to a monthly resolution with 12 samples per year using AnalySeries software (Paillard et al., 1996).

References

1. Paillard, D., Labeyrie, L., and Yiou, P. (1996) Macintosh program performtime-series analysis, *Eos Trans. AGU*, 77(39), 379.
2. Watanabe, T., Minagawa, M., Oba, T., Winter, A. (2001) Pretreatment of coral aragonite for Mg and Sr analysis: Implications for coral thermometers. *Geochemical journal*, 35(4): 265-269
3. Amiel, A. J., Miller, D. S. and Friedman, G. M. (1973) Incorporation of uranium in modern corals. *Sedimentology* 20, 523–528.

Chapter 3

Mekong River discharge and the East Asian monsoon recorded by a coral geochemical record from Con Dao Island, Vietnam

Abstract

The offshore flow of the Mekong River is strongly governed by the East Asian monsoon (EAM). Monthly-resolved skeletal carbonate Sr/Ca, Ba/Ca and oxygen isotope ($\delta^{18}O_c$) data from 1980 to 2005 of a *Porites* coral from Con Dao Island, ~90 km from the Mekong River mouth, were analyzed for capturing the past flood events and the signal of East Asian winter monsoon. Ba/Ca time series is characterized with intra-annual double peaks, the first large one in March during the dry season and relative small one in August during the wet season. The low values of seawater $\delta^{18}O$ ($\delta^{18}O_{sw}$), deduced from both the Sr/Ca ratio and $\delta^{18}O_c$, in the wet season resulted from precipitation and/or freshwater input from the Mekong River. The difference in the seasonal characteristics of Ba/Ca and $\delta^{18}O_{sw}$ between flood and no-flood years could be attributed to the seasonal reversal of the regional ocean current derived from the EAM.

Keywords: coral record; Ba/Ca; seawater oxygen isotope; Con Dao Island; Mekong River

1. INTRODUCTION

The Mekong River is one of the largest river systems in the world. The climate in the lower Mekong region is dominated by the East Asian monsoon. Precipitation occurs mainly during the warm/wet season from May to November. River discharge reaches a maximum in September or October and a minimum in April (based on averaged water discharge data from the Tan Chau station from 1979 to 2005). The Mekong River plume is mostly geostrophic and exhibits a strong seasonal variability related to the monsoon wind and water current system, which is northward in winter and southward in summer (Tang et al., 2006; Hein et al., 2013;

Unverricht et al., 2014). The Mekong River in Vietnam represents a great potential for agriculture and aquaculture production. However, the knowledge about Mekong River discharge and past flood events have been very limited because of the lack of observations and historical documents (Tran, 2009; Xue et al., 2012). The paleoclimatic history of Mekong River discharge will contribute to prevent the disaster due to floods and climate changes, and to promote economic development in the Mekong Delta.

The geochemical compositions of *Porites* coral skeletons are affected by the prevailing environment at the time of skeletal deposition and high-resolution geochemical analyses of the skeletons provide useful information about seasonal variations in past sea surface climates and environments (Watanabe et al., 2003). Coral skeletal Sr/Ca ratios have been used as a proxy for sea surface temperature (SST) (e.g. Mitsuguchi et al., 2008; Bolton et al., 2014). The coral stable oxygen isotopic record ($\delta^{18}O_c$) has also been used for the reconstruction of SST (Watanabe et al., 2003; Cahyarini et al., 2014). Using both the Sr/Ca ratio and $\delta^{18}O$, we can reconstruct the oxygen isotopic composition of sea water ($\delta^{18}O_{sw}$) as an indicator of sea surface salinity (SSS) related to freshwater runoff into the coral reefs. McCulloch et al. (1994) calculated $\delta^{18}O_{sw}$ and residual variation in coral $\delta^{18}O$ for the Great Barrier Reef of Australia. Their results were shown to correlate with the freshwater runoff from a nearby major river. This was used as proxy for the reconstruction of past flood events related to ENSO cycles in the western tropical Pacific corals.

Ba/Ca ratios in coral skeletons have been well calibrated with Ba concentration in seawater (La Vigne et al., 2016, Gonneea et al., 2017). Coral Ba/Ca ratios reflect changes in the seawater Ba/Ca composition due to oceanic upwelling, local rainfall, and suspended sediment flux associated with river discharge, land-use changes and coastal development (e.g. McCulloch et al., 2003, Montaggioni et al., 2006, Carriquiry and Horta-Puga, 2010, Horta-Puga and Carriquiry, 2012). McCulloch et al. (2003) indicated that the Ba/Ca ratios in coral skeletons

from the Great Barrier Reef increased five to ten-fold after the arrival of European's in Australia. They argued that the sediment load from the Burdekin River increased with soil erosion rate due to increasing cattle grazing and agricultural activity around its catchment area and influenced on the coral reef environment. Ba/Ca ratios in coral skeletons have been used as powerful recorder of sediment loading by river discharge in the various coral reefs such as Great Barrier Reef (Jupiter et al., 2008), the Gulf of Mexico (Carriquiry and Horta-Puga, 2010), and Madagascar (Maina et al., 2012). In this paper, we attempted to establish the relationship between Mekong River discharge, flood events and coral Ba/Ca ratios, reconstructed $\delta^{18}O_{sw}$ based on a 26 year-old *Porites* coral core from Con Dao Island, Southern Vietnam.

2. MATERIALS AND METHODS

2.1. Coral sampling

From 2 to 8 June 2006, we drilled cores (CD-4) from two *Porites* coral colonies living at 20 m depth on the southwest side of Con Dao Island, Vietnam (N 8°33.43' E 106°33'), which is located 90 km away from the Mekong Delta coast (Figure 3.1). The total length of the core was 150 cm and 5 cm in diameter. The coral cores were cut into 5-mm-thick slabs using a diamond saw blade along the axis of major growth. Each coral slab was ultrasonically cleaned 3 times with deionized water for 10 minutes to remove surface contaminants. Then, the coral slabs were dried in an oven at 40 °C for 48 h. The slabs were photographed under UV light and X-ray. The UV and X-ray photographs revealed luminescent bands and density bands on the coral skeletons, respectively (Figure 3.2). There were 82 bands in total, and all bands were clear. These bands were assumed to be annual growth bands covering the period AD 1924–2005. On the basis of the banding patterns in the UV-luminescence photograph and X-radiograph, measurement lines were determined on the coral slabs for sampling along the skeletal growth axis. A total of 1150 sub-samples were taken from 0.8 mm diameter drill spots at 1 mm intervals with a drilling depth of 1 mm. In this paper, we have already analyzed 398

sub-samples corresponding to the period from 1980 to 2005.

2.2. Oxygen isotope analysis

Coral oxygen isotope ratios were measured with an isotope ratio mass spectrometer (IRMS; Finnigan MAT 253) connected with a carbonate device (Kiel IV) at Hokkaido University. The 20 - 40 µg carbonate powder was reacted with 100% H_3PO_4 at 70 °C, and the emitted CO_2 gas was purified and introduced from the carbonate device to the IRMS. Oxygen isotope ratios are expressed as delta notation relative to Vienna Pee Dee Belemnite. The internal precision for $\delta^{18}O$ was 0.04 ‰ using replicate measurements of the NBS-19 standard (1σ, n = 80).

2.3. Trace element analysis

Trace element concentrations in the coral skeletons were measured with inductively coupled plasma-atomic emission spectrometry (ICP-AES; iCAP6200) at Hokkaido University. The sample solution for coral Sr/Ca ratio analysis was prepared using 80 - 90 µg sample powder dissolved in 0.5 ml HNO_3 25% and milli-Q water, adjusting the Ca concentration to 7 ppm.

For Ba/Ca analysis, the 115 - 128 µg powder sample was rinsed with 2 ml milli-Q water in an ultrasonic bath for 10 minutes for removing the possible organic contamination. The solution was then centrifuged for 15 minutes and 1.8 ml milli-Q water was removed. The residual solution was mixed with 0.5 ml HNO_3 25% and milli-Q water to adjust the Ca concentration to 9 ppm. The ultrasonic nebulizer was coupled to ICP-AES to detect trace amounts of barium. Measurement accuracy was monitored by analyzing the Porites coral standard JCp-1. Analytical precision of the Sr/Ca and Ba/Ca determinations was 0.07 % and 1.2 %, respectively.

2.4. Climate data

The monthly SST, SSS and precipitation (Figure 3.3) have been recorded since January 1980 at the Con Dao meteorological observation station (Institute of Hydrology and Meteorology of Vietnam), which is located approximately 15 km away from the coral sampling site.

2.5. Age model

We used the coral Sr/Ca ratios to create an age model for all proxies. Minima and maxima of the Sr/Ca ratios were tied to the maxima and minima of observed SST from Con Dao Island. The Sr/Ca data and instrumental SST were re-sampled to a monthly resolution with 12 samples per year using AnalySeries software (Paillard et al., 1996).

2.6. Data calculation

The seasonal variation of all proxies in period from 1980 to 2005 were calculated by using averaged data of each months during 26 years (Figure 3.4). And the standard error was showed as standard deviation values (σ) of the means of each months (Figure 3.4 and 3.5).

3. RESULTS AND DISCUSSION

3.1. Coral proxy calibrations

The coral Sr/Ca ratios and $\delta^{18}O$ showed 26 distinct annual cycles (Figure S2). The average of the Sr/Ca ratios was 8.90 (mmol/mol), with values ranging from 8.71 to 9.09 (mmol/mol). The $\delta^{18}O$ averaged -5.68 (‰VPDB) and ranged from -5.04 to -6.51 (‰VPDB). The calibration of the coral Sr/Ca thermometer was obtained from the linear least squares regression between the coral Sr/Ca maxima (minima) and the SST maxima (minima) at Con Dao station from 1980 to 2005 as below:

$$\text{Sr/Ca (mmol/mol)} = (-0.0504 \pm 0.004)*\text{SST (°C)} + (10.305 \pm 0.17)$$

($r^2 = 0.8108$, $P < 0.01$)

The slope of the Sr/Ca - SST regression was -0.0504 ± 0.004 mmol/mol/^oC, which lies within the range for slope values, from -0.0424 to -0.0608 mmol/mol/ °C, recorded in other Porites corals in the East China Sea, South China Sea and East Sea of Vietnam (Figure 3.6).

We established a regression line between the SST data from Con Dao Island and $\delta^{18}O$, assuming that $\delta^{18}O$ reflected only SST variations, as follows:

$$\delta^{18}O_c\ (‰_{VPDB}) = - 0.2207*SST\ (°C) + 0.4568$$

($r^2 = 0.8495$; $P < 0.01$)

Coral $\delta^{18}O$ is influenced by both SST and the $\delta^{18}O$ in seawater. The mean seasonal variation in SSS was approximately 6 ‰, with a maximum of 34 ‰ in February - April and a minimum of 28 ‰ in October. $\delta^{18}O_{sw}$ might be a significant contribution to coral $\delta^{18}O$. $\delta^{18}O_{sw}$ values was calculated from both the coral Sr/Ca ratio and $\delta^{18}O_c$. To isolate $\delta^{18}O_{sw}$, the SST component was removed from the $\delta^{18}O_c$ values using Sr/Ca-SST estimates (Cahyarini et al., 2014). The average calculated $\delta^{18}O_{sw}$ was approximately 0.11 (‰VPDB), and the values ranged between -1.01 to 0.97 ‰. The error of calculated $\delta^{18}O_{sw}$ was ± 0.11 ‰ (±σ) (Following Nurhati et al., 2011).

3.2. Factors controlling the Ba/Ca ratio

The coral Ba/Ca ratios varied from 2.51 to 8.45 (µmol/mol), with an average value of 3.7 (µmol/mol). The Ba/Ca ratios also showed seasonal variation with peaks typically occurring between January and March (Figure 3.3).

There is still much debate about the possible influence factors on coral Ba/Ca. The main influence factors that can affect the coral Ba/Ca ratio include: (1) SST, (2) seasonal upwelling, (3) “vital effects” including extension rates and phytoplankton blooms and (4) precipitation associated with river discharge and flood events.

SST has been known to be a thermodynamic driver regulating the incorporation of cations in corals and other marine carbonates. Previous studies reported the correlation between SST and the coral Ba/Ca ratio. Gaetani and Cohen (2006) suggested that barium incorporation into coral skeletal is inversely correlated with SST between 15 and 75°C. Moreover, Chen et al. (2011) showed that the maxima of coral Ba/Ca from Daya Bay, northern South China Sea, coincided with the winter minimum SSTs. However, in our study, we compared coral Ba/Ca values with SST from Con Dao Island and found that there was no association with SST, only a weak correlation ($r = 0.003$, $n = 398$, $P < 0.001$) (Figure 3.3). Therefore, our results suggest that SST did not significantly affect coral Ba/Ca ratios.

Previous studies were successful in using coral Ba/Ca ratios as a proxy for seasonal upwelling (Montaggioni et al., 2006). Upwelling is a regular phenomenon during summer (June to September) in the continental shelf of the East Sea in Vietnam (ESVN). Upwelling events along the coast of Vietnam are driven by the southwest monsoon, which causes strong seasonal winds parallel to the coast. The upwelling appears along the coast, ~270 km distance from Con Dao Island (Hu and Wang, 2016)(Figure 3.7). Moreover, our Ba/Ca peaks mostly occurred in cold winters (March) and not in the upwelling season (June to September). Furthermore, there is no evidence showing upwelling can affect the coral in Con Dao Island.

The underlying principle for inferring palaeoenvironmental conditions from coral geochemistry is the assumption that coral physiology does not pose random influence upon the chemical composition of the skeleton. However, coral geochemistry might be modulated by biological influences (termed as ‘vital effects’) that affect the utility of coral skeleton for environment monitoring purposes. Gaetani and Cohen (2006) indicated “vital effects” accompanying coral growth influences on Ba incorporation in corals. In our core, the coral extension rates show quite stable through the 26 years, on average 12 mm/year with a range between 11 to 14.2 mm. In this study, we compared between annual growth rate and averaged

Ba/Ca ratios in each years during period from 1980 to 2005. The result showed the weak positive correlation between them ($r = 0.242$, $n = 26$). Therefore, we assumed that coral growth rates did not significantly affect this coral record. Tang et al. (2006) demonstrated the major offshore phytoplankton bloom appear in the Gulf of Thailand during the winter northeast monsoon season and in the Vietnam East Sea during the summer southwest monsoon season. Phytoblankton blooms will combine with Mekong River discharge and influence on coral around our study area. Although complicated factors may influenced on coral Ba/Ca proxy, average seasonal profile of Ba/Ca ratios from 26 year records would eliminate or minimize noise due to other controlling factors.

In the coastal area, barium in coral skeletons mainly has been used as a record of terrestrial runoff (Prouty et al., 2010). Sediments derived from Mekong Delta soils with a high rate of weathering and biological activities are usually rich in Ba. When these sediments are transported by river into coastal environments, Ba is desorbed from the sedimentary particles and released into the dissolved phase of seawater. Thus, the Ba/Ca ratios from coral in coastal areas can be used as a proxy for river discharge. In addition, the volume of freshwater flow from the mainland to coastal areas is highly dependent on rainfall, and the levels of coastal Ba increase with increases in river outflow, meaning that the coral Ba/Ca record could be used as a tracer of precipitation. Sinclair and McCulloch (2004) suggested that peaks in Ba/Ca ratios from coral in the Great Barrier Reef coincided with observed river flood plumes and local rainfall. Since Con Dao Island is close to the mouth of the Mekong River and Unverricht et al. (2008) show that Con Dao Island is strongly influenced by the Mekong River discharge, which causes high suspended sediment concentrations and phytoplankton blooms around the island (Tang et al., 2006). Our Ba/Ca profiles showed the variation corresponding the seasonal discharge from Mekong River therefore Ba/Ca variation in the coral skeletons is also

predominately controlled by terrestrial inputs from the Mekong River Delta and reflects the suspended sediment associated with Mekong River discharge.

3.3. Seasonal characteristics of coral geochemical records

We calculated the seasonal variation of all proxies in the period 1980 - 2005 and compared it with climatological data from Con Dao Island (Figure 3.4). Sr/Ca ratios show maxima and minima in May and January corresponding to observed SST. The maximum of $\delta^{18}O_{sw}$ was determined to occur in May when SST and SSS are at a maximum, and the minimum of $\delta^{18}O_{sw}$ occurred in the rainy season because of the high amount of precipitation or freshwater input from the Mekong River. We can see the appearance of two peaks in the annual variation of the coral Ba/Ca ratio. The higher peak of 4.24 µmol/mol (±1.25) occurred in March (Winter), and the lower one of 3.72 µmol/mol (±0.67) occurred in August (Summer) when the precipitation was the highest.

Both of the peaks in the Ba/Ca profile could reflect the river sediment discharge corresponding to the cool/dry season and warm/wet season, respectively (McCulloch et al., 2003). However. the peak in August was lower than the one in March, which means that although the river discharge reached a maximum in summer, the effect of the suspended sediment on Con Dao Island's corals was not significant. The Ba/Ca ratios calculated in this research were compared with the annual river discharge recorded at the Tan Chau station (N 10°48', E 105°13') on the Mekong River and precipitation recorded at Con Dao Island meteorological station during the period from 1980 to 2005. There was a weak correlation between them with $r^2 = 0.0252$ and $r^2 = 0.0214$, respectively. This suggested that river discharge and local rainfall did not have a direct influence on Con Dao Island corals. To explain the difference between the effect of suspended sediment associated with river discharge, we considered the seasonal sediment transport model of the Mekong River related to the East Asian monsoon as follows (Figure S5): during the high flow season (May–October), a considerable part

of riverine sediment was delivered to the Mekong River mouth and temporally deposited there; then during the low flow season (November–April), the previously deposited sediment was resuspended by strong mixings associated with the strong northeast monsoon and subsequently transported southwest along-shelf by coastal circulation (Hein et al., 2013). The monsoon wind had an important role in changing the surface water current and sediment transportation in this area. The amount of suspended sediment effect on Con Dao Island in winter is higher than in summer. This is consistent with the results of our determined coral Ba/Ca ratio from Con Dao Island.

3.4. Influence of flood events related to Mekong River discharge and East Asian monsoon on coral records.

Ba/Ca and $\delta^{18}O_{sw}$ could also be used to reconstruct past flood events. We investigated historical documents about flood history in the Mekong Delta. During 1980 - 2005, seven large flood events were found in 1984, 1991, 1994, 1996, 2000, 2001 and 2002 (Tran, 2009). We calculated the seasonal variation of Ba/Ca and $\delta^{18}O_{sw}$ separately in flood years and no-flood years (Figure 3.5). We found a significant increase of the Ba/Ca ratios and a decrease of $\delta^{18}O_{sw}$ in the warm/wet season in flood years. These seasonal characteristics correspond to larger amounts of freshwater discharge from the Mekong River when a flood occurred or a high amount of precipitation in the warm/wet season related to the East Asian summer monsoon. Our coral Ba/Ca and $\delta^{18}O_{sw}$ from Con Dao Island could be used as a possible proxy for capturing the past flood events in the Mekong Delta.

4. CONCLUSIONS

Our results suggested that the Mekong River discharge was influenced by the seasonal migration of the Asian monsoon and ocean currents. The maximum discharge of freshwater from the river reached our coral site in summer (from May to November), however the sediment discharge model of the Mekong River indicated the amount of suspended sediment influencing

on Con Dao Island was high in winter (from December to April). Coral Ba/Ca record in Con Dao Island reflected the sediment discharge from the Mekong River. On the other hand, Ba/Ca and $\delta^{18}O_{sw}$ could be used as indicators of flooding from the Mekong Delta. During the period from 1980 to 2005, the difference in seasonal characteristics of geochemical signals in flood years and no-flood years was detected. During the flood years, in the warm/wet season, the Ba/Ca ratio and $\delta^{18}O_{sw}$ data significantly increased and decreased, respectively. These results reflect the increase in the Mekong River freshwater discharge and the sudden increase of precipitation when floods occurred in warm/wet season.

References

1. Bolton, A., Goodkin, N.F., Hughen, K., Osterman, D.R., Vo, S.T., Phan, H.K. (2014) Paired Porites coral Sr/Ca and $\delta^{18}O$ from the western South China Sea: Proxy calibration of sea surface temperature and precipitation. *Palaeogeography, Palaeoclimatology, Palaeoecology* 410, 233–243.
2. Cahyarini, S.Y., Pfeiffer, M., Timm, O., Dullo, W.C., Schönberg, D.G. (2008) Reconstructing seawater $\delta^{18}O$ from paired coral $\delta^{18}O$ and Sr/Ca ratios: methods, error analysis and problems, with examples from Tahiti (French Polynesia) and Timor (Indonesia). *Geochimica et Cosmochimica Acta* 72, 2841–2853.
3. Carriquiry, J.D., Horta-Puga, G. (2010) The Ba/Ca record of corals from the Southern Gulf of Mexico: contributions from land-use changes, fluvial discharge and oil-drilling muds. *Marine Pollution Bulletin* 60, 1625–1630.
4. Chen, T., Yu, K., Li, S., Chen, T., Shi, Q. (2011) Anomalous Ba/Ca signals associated with low temperature stresses in Porites corals from Daya Bay, northern South China Sea. *Journal of Environmental Sciences* 2011, 23(9), 1452–1459.

5. Gaetani, A.G., Cohen, L.A. (2006) Element partitioning during precipitation of aragonite from seawater: A framework for understanding paleoproxies. *Geochimica et Cosmochimica Acta* 70, 4617–4634.
6. Gonneea, E.M., Cohen, L.A., DeCarlo, M.T., Charette, A.M. (2017) Relationship between water and aragonite barium concentrations in aquaria reared juvenile corals. *Geochimica et Cosmochimica Acta* 209, 123–134.
7. Hein, H., Hein, B., Pohlmann, T. (2013) Recent sediment dynamics in the region of Mekong water influence. *Global and Planetary Change* 110, 183–194.
8. Horta-Puga, G., Carriquiry, J.D. (2012) Coral Ba/Ca molar ratios as a proxy of precipitation in the northern Yucatan Peninsula, Mexico. *Applied Geochemistry* 27, 1579–1586.
9. Hu, J., and Wang, X.H. (2016) Progress on upwelling studies in the China seas, *Reviews of Geophysics*, 54, 653–673.
10. Jupiter, S., Roff, G., Marion, G., Henderson, M., Schrameyer, V., McCulloch, M., Hoegh-Guldberg, O. (2008) Linkages between coral assemblages and coral proxies of terrestrial exposure along a cross-shelf gradient on the southern Great Barrier Reef. *Coral Reefs* 27, 887–903.
11. Lavigne, M., Grottoli, A.G., Palardy, J.E., Sherrell, R.M. (2016) Multi-colony calibrations of coral Ba/Ca with a contemporaneous in situ seawater barium record. *Geochimica et Cosmochimica Acta* 179, 203-216.
12. Maina, J., Moel, H., Vermaat, J., Bruggemann, H., Guillaume, M., Grove, C., Madin, J.S., Mertz-Kraus, R., Zinke, J. (2012). Linking coral river runoff proxies with climate variability, hydrology and land-use in Madagascar catchments. *Marine pollution bulletin* 64, 2047-2059.

13. McCulloch, M.T., Fallon, S., Wyndham, T., Hendy, E., Lough, J., Barnes, D. (2003) Coral record of increased sediment flux to the inner Great Barrier Reef since European settlement. *Nature* 421, 727–730.
14. McCulloch, M.T., Gagan, M.K., Mortimer, G.E., Chivas, A.R., Isdale, P.J. (1994) A high-resolution Sr/Ca and $\delta^{18}O$ coral record from the Great Barrier Reef, Australia, and the 1982–1983 El Nino. *Geochim. Cosmochim. Acta* 58, 2747–2754.
15. Mitsuguchi, T., Dang, P.X., Kitagawa, H., Uchida, T., Shibata, Y. (2008) Coral Sr/Ca and Mg/Ca records in Con Dao Island off the Mekong Delta: Assessment of their potential for monitoring ENSO and East Asian monsoon. *Global and Planetary Change* 63, 341–352.
16. Montaggioni, L.F., Le Cornec, F., Corrège, T., Cabioch, G. (2006) Coral barium/calcium record of mid-Holocene upwelling activity in New Caledonia, South-West Pacific. *Palaeogeography, Palaeoclimatology, Palaeoecology* 237, 436–455.
17. Nurhati, I.S., Cobb, K.M., Di Lorenzo, E. (2011) Decadal-scale SST and salinity variations in the central tropical Pacific: signatures of natural and anthropogenic climate change. *Journal of Climate*, 24 (13), 3294–3308.
18. Paillard, D., Labeyrie, L., and Yiou, P. (1996) Macintosh program performtime-series analysis, *Eos Trans. AGU*, 77(39), 379.
19. Prouty, N.G., Field, M.E., Stock, J.D., Jupiter, S.D., McCulloch, M. (2010) Coral Ba/Ca records of sediment input to the fringing reef of the southshore of Moloka'i, Hawai'i over the last several decades. *Marine Pollution Bulletin* 60, 1822–1835.
20. Sinclair, D.J., McCulloch, M.T. (2004) Corals record low mobile barium concentrations in the Burdekin River during the 1974 flood: evidence for limited Ba supply to rivers? *Palaeogeography, Palaeoclimatology, Palaeoecology* 214, 155–174.
21. Tang, D.L., Kawamura, H., Shi, P., Takahashi, W., Guan, L., Shimada, T., Sakaida, F., Isoguchi, O. (2006) Seasonal phytoplankton blooms associated with monsoonal influences

and coastal environments in the sea areas either side of the Indochina Peninsula. *Journal of Geophysical Research* 111, G01010, doi:10.1029/2005JG000050.

22. Tran, N.H. (2009) Some typical floods and flooding zoning in the Mekong Delta. *Collection of Science and Technology: 50 years of Construction and Development,* volume II, 89-100.
23. Unverricht, D., Nguyen, T.C., Heinrich, C., Szczucinski, W., Lahajnar, N., Stattegger, K. (2014) Suspended sediment dynamics during the inter-monsoon season in the subaqueous Mekong Delta and adjacent shelf, southern Vietnam. *Journal of Asian Earth Sciences* 79, 509–519.
24. Watanabe, T., Gagan, M.K., Corrége, T., Gagan, H.S.,Cowley, J., Hantoro, W.S. (2003) Oxygen isotope systematics in Diploastrea heliopora: New coral archive of tropical paleoclimate. *Geochimica et Cosmochimica Acta* 67, 1349–1358.
25. Xue, Z., He, R., Liu, J.P., Warner, J.C. (2012) Modeling transport and deposition of the Mekong River sediment. *Continental Shelf Research* 37, 66–78.

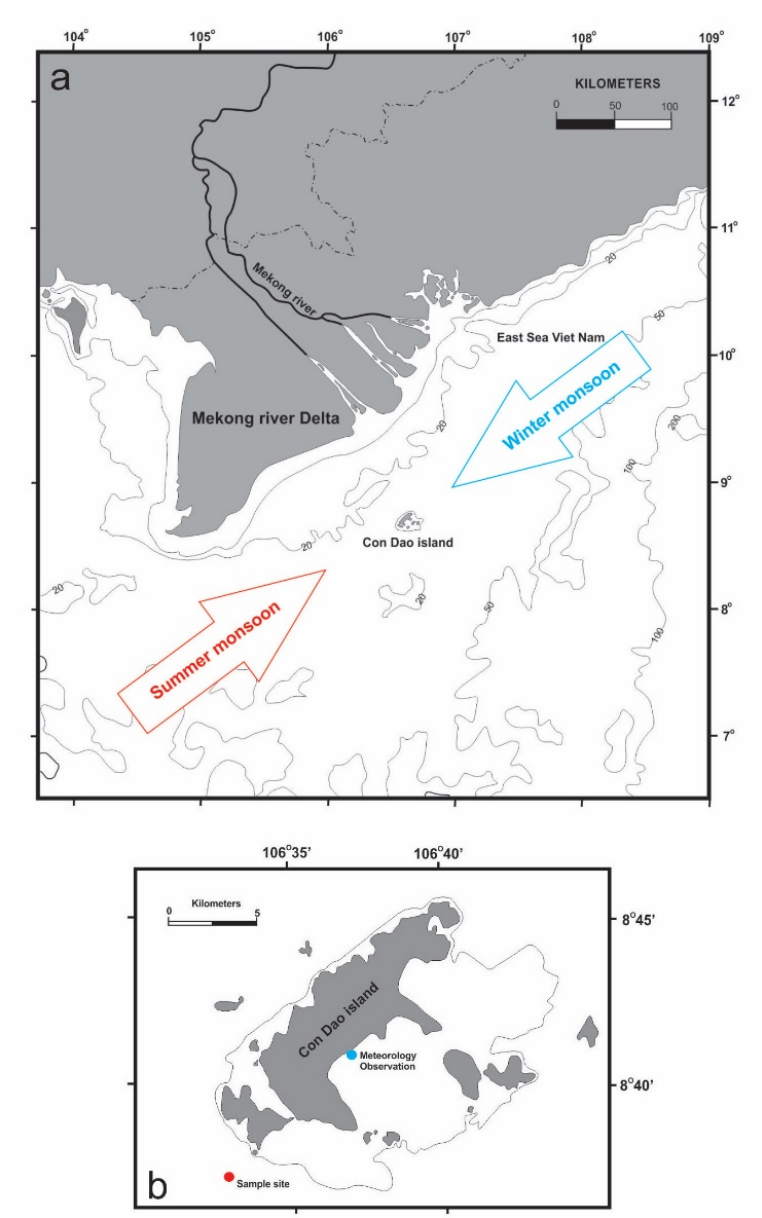

Figure 3.1. (a) Location of the East Sea and Mekong River of Vietnam. The climate of this area is strongly dominated by the East Asian monsoon: summer monsoon and winter monsoon correspond to southwesterly winds and northeasterly winds, respectively. Con Dao Island located in the ESVN, ~ 90 km from the mouth of the Mekong River. (b) Map of Con Dao Island showing the location of the sampling site at the southwest side of the island (red circle). Meteorological observation station (blue circle) located 15 km distance away from the sampling site.

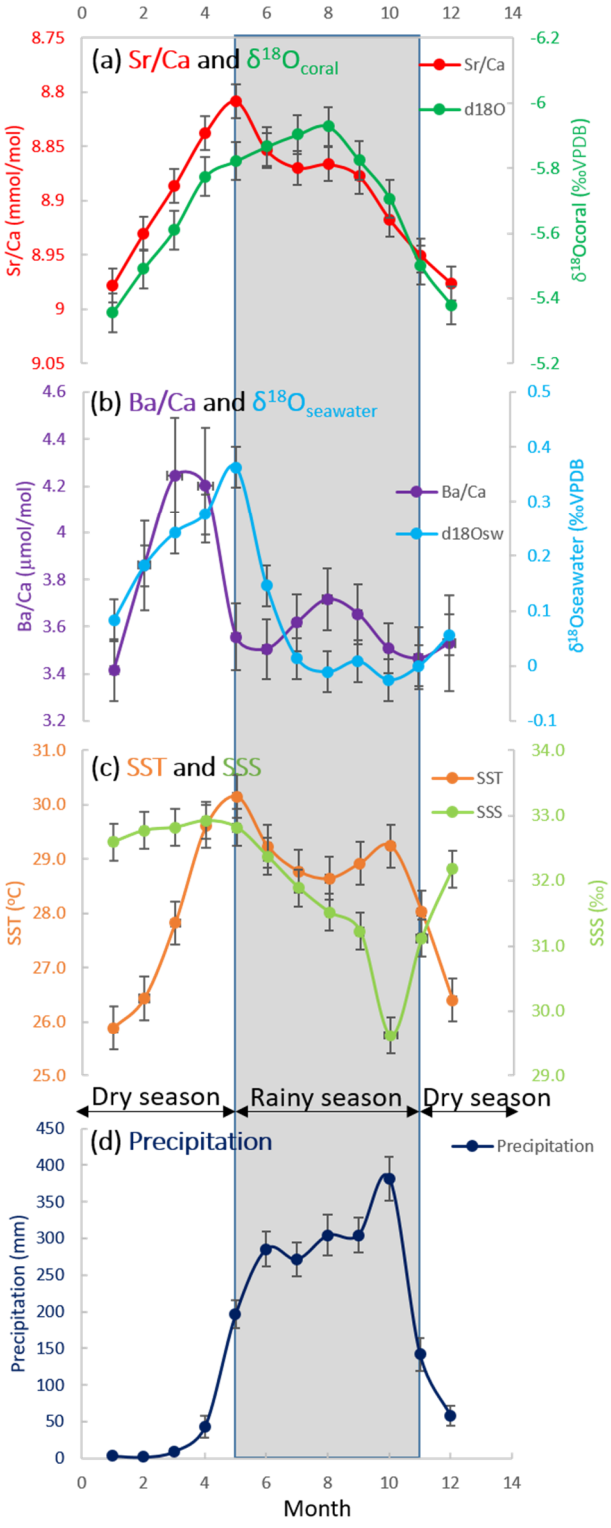

Figure 3.4. Seasonal characteristics of (a) Sr/Ca ratios and $\delta^{18}O_{coral}$; (b) Calculated $\delta^{18}O_{seawater}$ and Ba/Ca ratio and climatological data calculated from monthly data; (c) SST and SSS and (d) precipitation in the period from 1980 to 2005. Error bars indicate standard error.

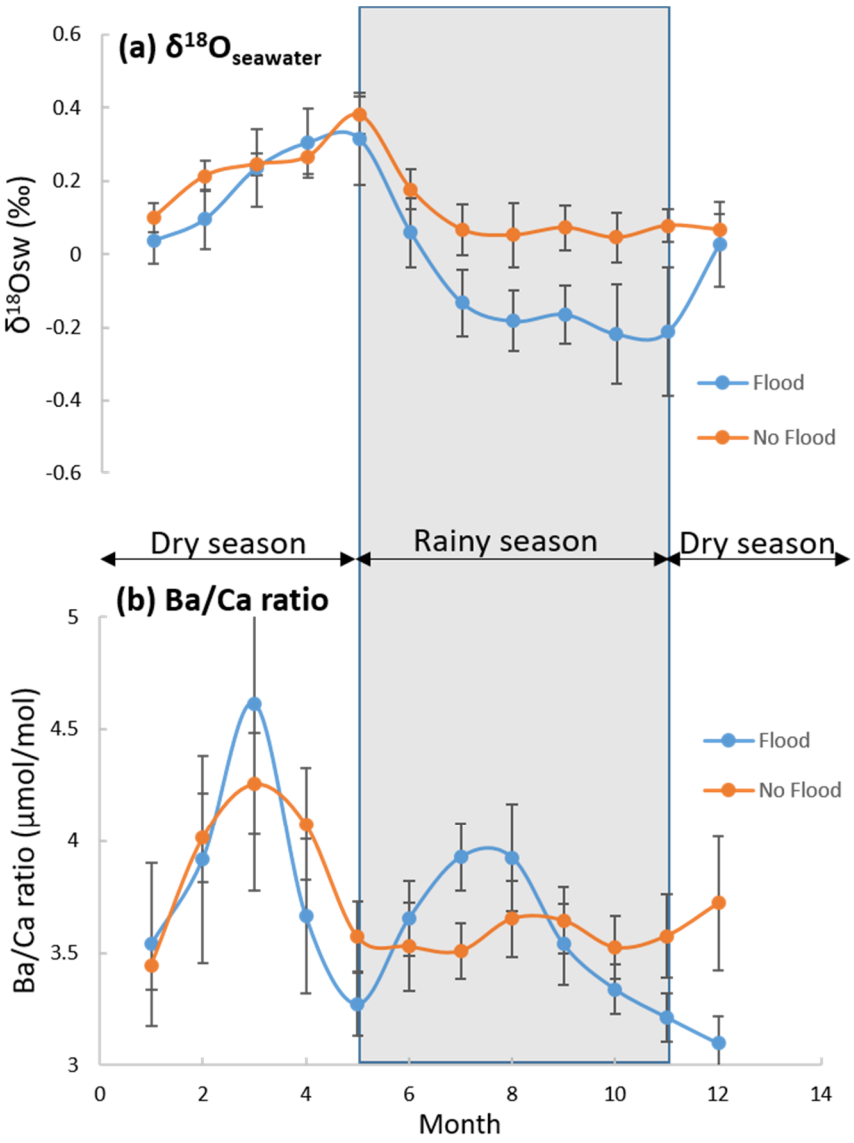

Figure 3.5. The comparison between monthly averages of calculated (a) $\delta^{18}O_{seawater}$ and (b) Ba/Ca ratios during the period from 1980 to 2005, separated into flood years and no-flood years. Error bars indicate standard error.

Tables

No	Study	Location	b	a	Species	r^2
1	Mitsuguchi et al. (1996)	Ishigaki island, ECS – Pacific	10.543	-0.0608	*Porites lutea*	0.728
2	Shen et al. (1996)	Taiwan, SCS	10.307	-0.0505	*Porites lutea*	0.91
3	Wei et al. (2000)	Hainan island, SCS	10.600	-0.0504	*Porites lutea*	0.56
4	Yu et al. (2005)	Leizhou Peninsula, SCS	9.836	-0.0424	*Porites lutea*	N.A
5	Sun et al. (2005)	Xisha island, ESVN	10.327	-0.0534	*Porites sp.*	0.96
6	Mitsuguchi et al. (2008)	Con Dao island, ESVN	10.105	-0.0446	*Porites sp.*	0.951
7	This study (2017)	Con Dao island, ESVN	10.305	-0.0504	*Porites sp.*	0.810
8	A. Bolton et al. (2014)	Hon Tre island, ESVN	10.573	-0.055	*Porites sp.*	0.75

Table 1. *Some of the Sr/Ca vs temperature calibration equations for Porites coral skeletons collected from the South China Sea, East China Sea and East Sea Vietnam expressed in the form of Sr/Ca (mmol/mol) = a x SST (°C) + b*

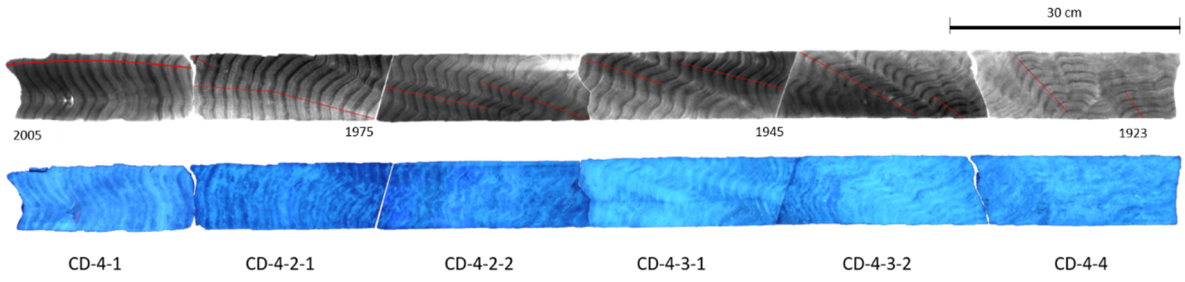

Figure 3.2. X-radiograph (top) and UV-luminescence photograph (bottom) of a coral skeletal core slab (Porites sp.) from Con Dao Island showing annual bands for AD 1922 - 2005. The UV photograph and X-ray photograph revealed clear luminescent banding and density banding in the

coral, respectively. One year is represented by high-density/low-density couplet. The red lines indicate the measurement lines for geochemical analysis. The scale bars are 30 cm.

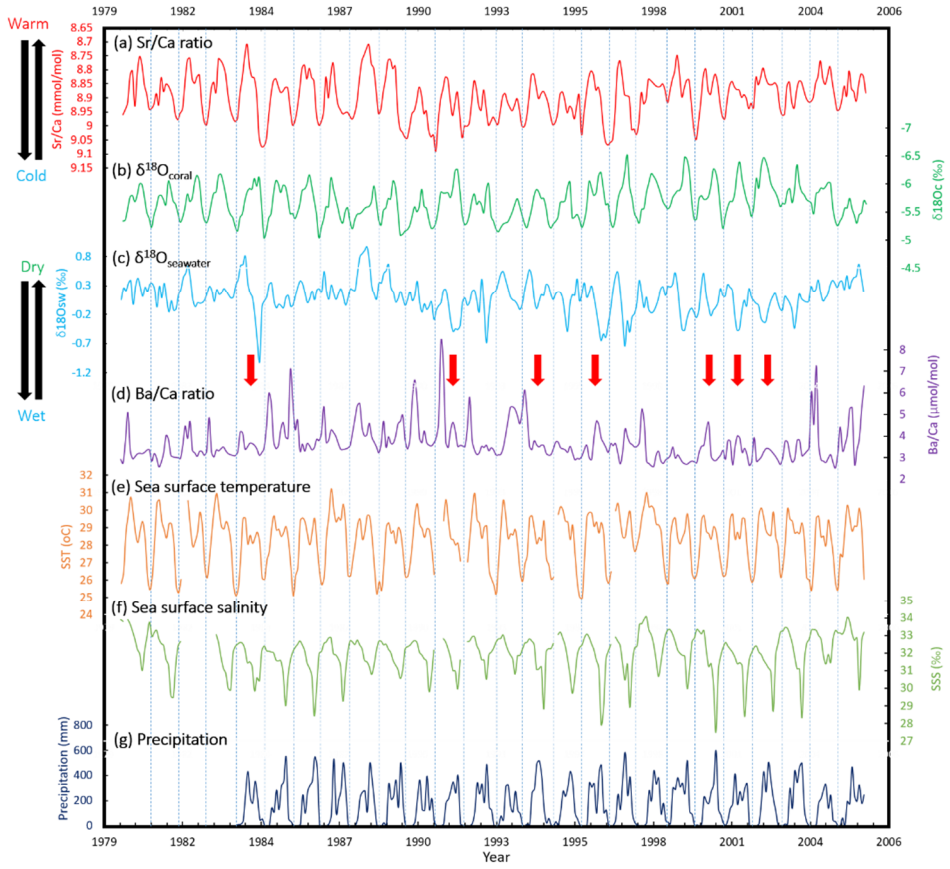

Figure 3.3. Comparison between geochemical records of Porites coral from Con Dao Island and monthly climate data recorded by a meteorological observation station in Con Dao Island during the period from 1980 to 2005. (a) Coral skeletal Sr/Ca ratio record, (b) coral skeletal $\delta^{18}O_c$ record, (c) calculated $\delta^{18}O_{sw}$, (d) coral skeletal Ba/Ca ratio, (e) SST, (f) SSS and (g) precipitation. Red arrows indicate the years that big floods occurred.

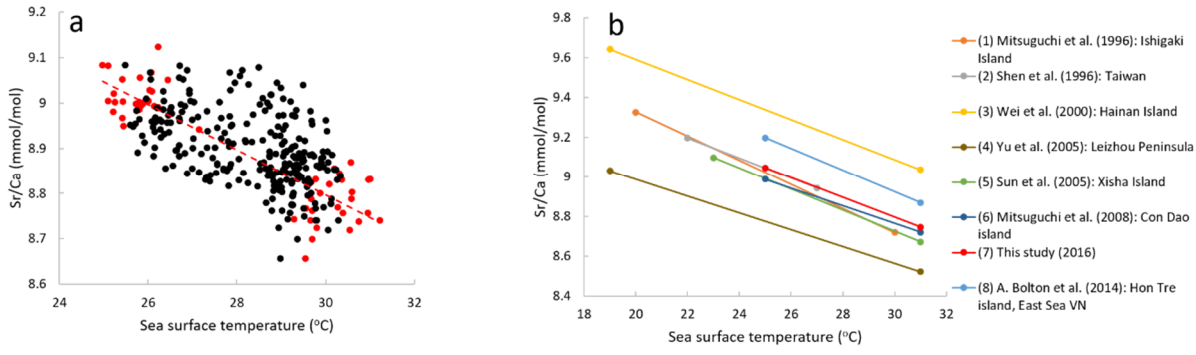

Figure 3.6. (a) Linear least squares regression of the Sr/Ca ratio and SST for Porites coral in Con

Dao Island using only annual extreme values (red circles) over the period from 1980 to 2005. Black circles are all measured values. (b) A compilation of Sr/Ca - SST thermometer readings in Porites corals from different areas. This study shows a similar slope with other studies.

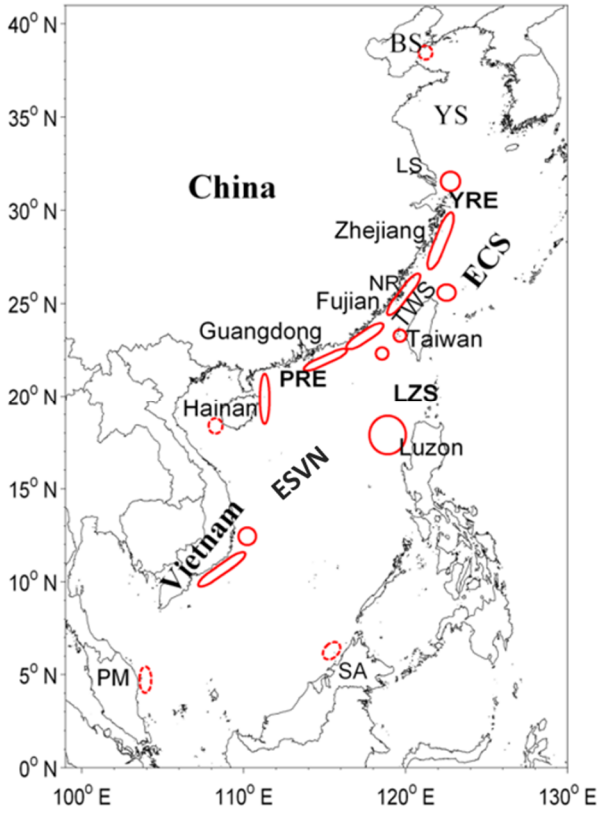

Figure 3.7. Map of China seas and the neighboring region. The red ellipses or circles schematically illustrate the dimensional structure of the cold eddy locations of the major upwelling regions (Hu and Wang, 2016)

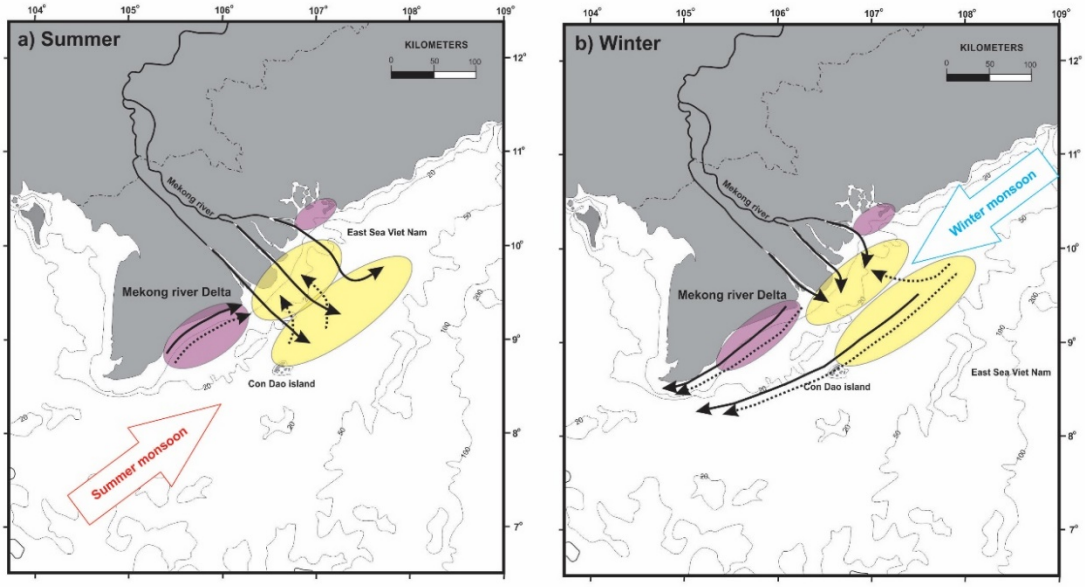

Figure 3.8. Suspended sediment transportation in the Mekong River, with a) representing for the high discharge season (southwest monsoon), b) representing for the low discharge season (northeast monsoon). Purple circles indicate erosion, yellow areas indicate deposition. Black arrows show the near surface pathways of sediment, dashed arrows show the near bottom transports of sediment.

Chapter 4

Fluctuation of the Ba/Ca record in Porites coral from Con Dao island during the period 1924 to 2005

1. Coral Ba/Ca variablity during 1924 to 2005

The change of Ba/Ca ratio in the coral skeleton could reflect the change of Ba concentration in the ambient seawater during the coral growth process. In addition, the concentration of Ba in the seawater is strongly influenced by river input into the coastal areas. Therefore, coralline Ba/Ca has been used as a geochemical proxy for flux of suspended sediment into coastal waters from rivers and associated with land-use changes (McCulloch et al., 2003; Moyer et al., 2012; Prouty et al., 2010). Coral Ba/Ca record in Con Dao Island in period from 1980 to 2005 can be used to reflect the sediment discharge from the Mekong River. I found the appearance of two peaks in the annual variation of the coral Ba/Ca ratio. The higher peak occurred in March (Winter), and the lower one occurred in August (Summer) when the precipitation was the highest. This consistent with the suspended sediment transportation model of Mekong river as follow: The maximum discharge of freshwater from the river reached coral site in summer (from May to November), however because of influence from the East Asin winter monsoon and ocean currents, the amount of suspended sediment influencing on Con Dao Island was high in winter (from December to April).

Variation of the Ba/Ca ratios from 1924 to 2005 was shown in figure 4.1. The observed range of Ba/Ca ratios of Porites coral from the Con Dao Island varied from 2.23 to 19.37 μmol mol^{-1}, with an average value of 3.60 μmol mol^{-1}. The maximum and minimum values appeared in 1953 and 1955, respectively. The Ba/Ca ratios also showed seasonal variation with peaks typically occurring in Winter (December to April). The fluctuation of Ba/Ca ratios reflected the changes of suspended sediment discharge from Mekong River during the period from 1924 to 2005. The amount of suspended sediment associated with the Mekong River discharge may be influenced by

the following factors: (1) Land use changes (e.g. deforestation, population growth), (2) Hydropower dams construction and (3) Indochina war.

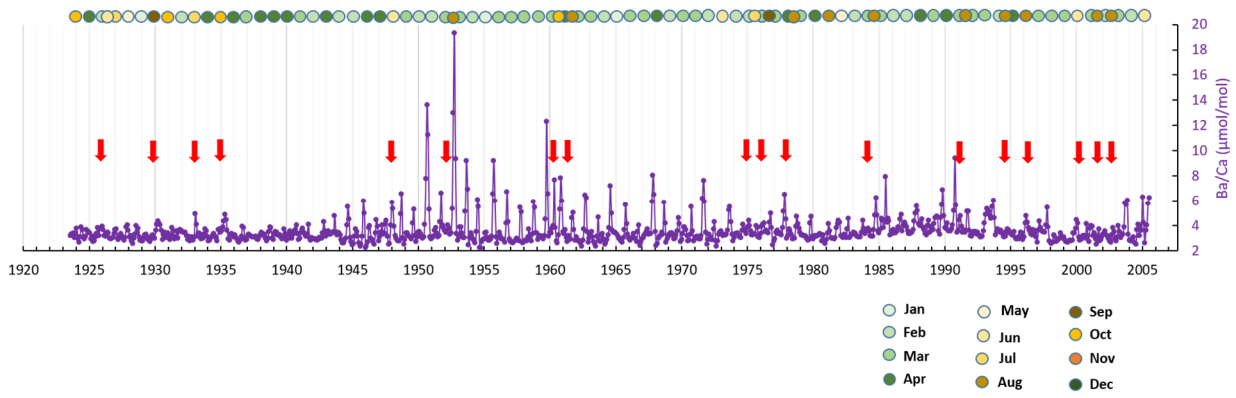

Figure 4.1. Variation of coral Ba/Ca record from Con Dao island during period from 1924 to 2005. The peaks typically occur in Winter (December to April) and sometimes in Summer mainly August to September when flood events usually occur in Mekong Delta. Red arrows indicate possible occurred flood events (1924 to 1979) and history-based occurred flood events (1980 to 2005)

The transboundary Mekong river basin (Figure 4.2) has a total area of 795 000 km^2, ranking it the 21st largest river basin worldwide, distributed between China (21%), Myanmar (3%), most of the territories of Lao PDR and Cambodia lie almost entirely within the basin with 25% and 20% respectively, Thailand (23%) and Viet Nam (8%) (MRC, 2005). The Mekong river basin can be divided into two parts: the "Upper Mekong basin" in China, and the "Lower Mekong basin" from Yunnan downstream to the East Sea of Viet Nam (ESVN). The upper basin (including China and Myanmar) contributes 18% of the water and approximately 50 % of the sediment that flows into the Mekong River. And Lower basin (including Lao PDR, Cambodia, Thailand and Viet Nam) contributes 82% of water and about 50% of sediment into the river.

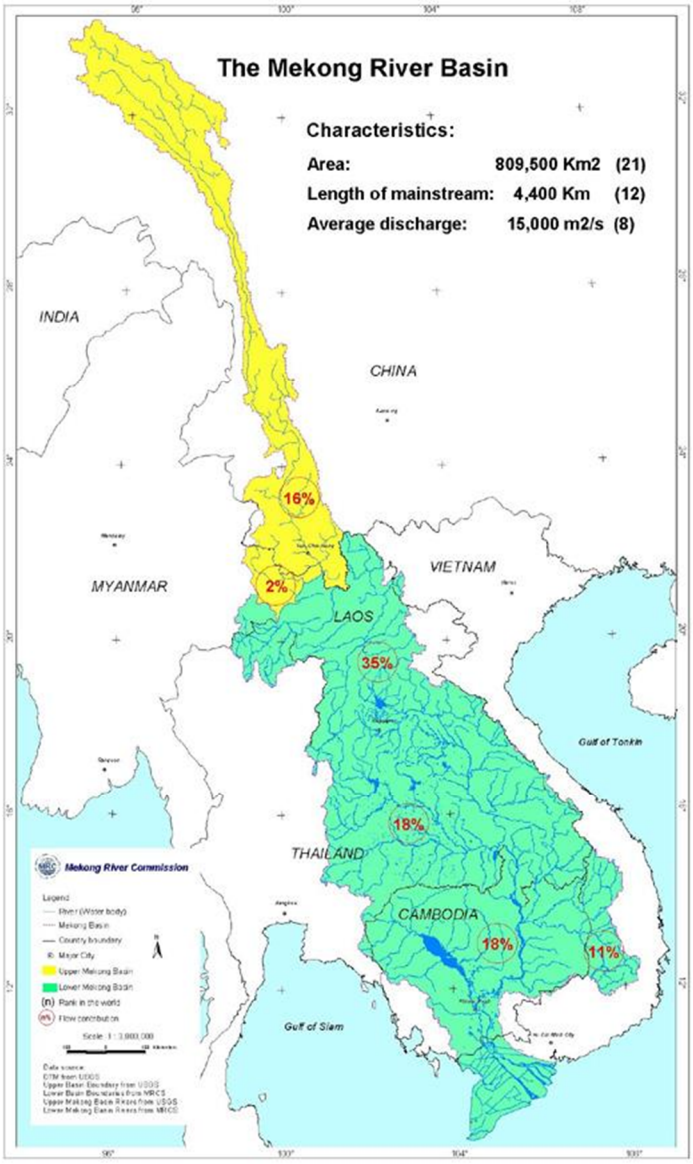

Figure 4.2. Mekong River basin (*Source: Mekong River Commission*)

The land-use change, which can be defined as the physical change in land cover over time caused by human action on the land (Turner and Meyer, 1994). Land use and soil cover are considered the most important factors affecting the intensity and frequency of overland flow and surface wash erosion (García-Ruiz, 2010). Soil erosion in river basin area leads to an increase of sediment in water river and suspended sediment discharge to the ocean. Many studies confirm the relationships between deforestation, agriculture and soil erosion. Conversion of forest and grasslands into agricultural land is one of the main reason of soil erosion. Forest provides a good

protection against surface runoff and soil erosion. Agriculture has caused a 7-fold increase in surface runoff and 21-fold increase in soil erosion (McDonald et al., 2002). In the Lower Mekong basin, land-use changes occurred over the past several decades. The Mekong River Basin population is over 70 million and is expected to increase rapidly (MRC, 2006). Nearly 80% of the region's population lives mainly by agriculture, fisheries and forest extraction. The expansion of commercial agriculture is considered the primary driver of deforestation in lower basin. Thailand lost at least half of forest cover since the early 1960s, the highest of all the lower Mekong countries. Between 1961 and 1989, Thailand's agricultural land increased by 13.12 million ha, while its forest area fell by 13.6 million ha (Cropper et al., 1999). On the Khorat Plateau region, which includes the Mun and Chi tributary systems, forest cover was significantly decreased from 42% in 1961 to 13% in 1993. Laos lies almost entirely within the lower Mekong basin. The area of agricultural land in Laos has increased significantly from about 700000 ha in 1982 to about 1.2 million ha in 2002, while the natural forest of Laos has been steadily reduced during the last three decades by shifting agriculture and permanent agriculture, dropped dramatically from 17 million ha in 1940 to 11.6 million ha in 1982 and 9.8 million ha in 2002 (Phimmavong et al., 2010). In the 1960s Cambodia has had higher percentage of the forest cover than any other country in lower Mekong river basin with a forests cover of 13.2 million ha, or 75% of the country. However, Cambodian forest cover has reduced dramatically in recent decades, with 65% in 1985, 62% in 1996/1997 and now is only 8.7 million ha (ODC, 2015). The Mekong delta in Vietnam is farmed intensively and has little natural vegetation left. Forest cover is less than 10 percent. In the Central Highlands of Vietnam, forest cover was reduced from over 95 percent in the 1950s to around 50 percent in the mid-1990s (MRC, 2005). So, the forest area in the lower Mekong basin countries were reduced significantly, it increases the likelihood of erosion, soil leaching, therefore the sediment discharge from Mekong River to ESV will be increased associated with high concentration of barium.

Country	Forest area 2015 (ha)	Forest cover 2015	Annual change in forest area (%)			
			1990-2000	2000-2010	2010-2015	1990-2015
Cambodia	9,457,000	54%	-1.1%	-1.3%	-1.3%	-1.2%
Lao PDR	18,761,000	81%	-0.7%	0.8%	1.0%	0.2%
Thailand	16,399,000	32%	2.0%	-0.5%	0.2%	0.6%
Vietnam	14,773,000	48%	2.3%	1.9%	0.9%	1.8%

Table 4.1. Forest cover changes in lower Mekong river basin countries (FAO, 2015)

The Mekong river basin has become one of the most active regions in the world for hydropower development with many more dams planned and under construction (MRC, 2009b). China constructed eight hydropower dams on the Mekong mainstream since 1995 and there were 133 proposed hydropower dams for the Lower Mekong River and tributaries. The predam sediment flux of the Mekong River into the South China Sea has been estimated at approximately 160 million tonnes per year (Mt yr-1), of which about half was produced by the upper of the basin area, the Lancang drainage in China (Milliman and Syvitski, 1992; Gupta and Liew, 2007; Walling, 2008). Dams have multiple environmental impacts, including changes in sediment load and channel form, reservoir-induced seismicity, short and long-term, economic and social effects of displacing riparian populations, and alterations of river ecology (Williams and Wolman, 1984). Reservoir of dams will trap all the bedload (the coarse sand and gravel moved along the river bed) and a percentage of the suspended load (the sand and finer sediment carried in the water column, held aloft by turbulence). Therefore, the supply of sediment to the river downstream and sediment discharge to ESVN will be reduced. Under a ‘‘definite future’’ scenario of 38 dams (built or under construction), Kondolf et al. (2014) calculated the cumulative sediment reduction to the Mekong Delta would be 51%. Under full build-out of all planned dams, cumulative sediment trapping will be 96%. That is, once in channel stored sediment is exhausted, only 4% of the predam sediment load would be expected to reach the Mekong Delta of Viet Nam. Moreover, the hydropower dams

construction contributed in deforestation (large areas of forest have been flooded with water) and buiding materials contribute as a part of sediment to Mekong River.

The Indochina wars were the conflict between Viet Nam, Laos, Cambodia with the involvement of France (1945-1954) and later the United States (beginning in the 1950s and finishing in April 1975). The wars are called the First Indochina war and the Second Indochina war (or Viet Nam war). The wars had a significant impacts on the environment of three Indochina countries such as: land and river system were destroyed, forests were burned… Especially in the period from 1954 to 1975, the United States has dropped tons of bombs to Viet Nam, Laos and Cambodia as follow: 3.770.000 tons in the southern and 937.000 tons in the northern of Viet Nam, 2.109.000 tons in south boundary and 321.000 tons in the northern of Laos, 685.000 tons in Cambodia. There were 7.882.547 tons in total, more than three times the United States used in World war II (extracted from "History of Vietnam Communist Party", published 2008). This led to increasing of soil erosion, the volume of soil and sediment in intertwined river system of lower Mekong river basin. Therefore increasing the sediment discharge to ESVN.

In summary, the facters related to human activities such as: land-use areas changes, construction of hydropower dams and wars, has a significant role in environment changes of Mekong river basin, particularly the sediment discharge of Mekong River to ESVN. This contributed in the fluctuation of coral Ba/Ca from Con Dao island, in front of Mekong river mouth.

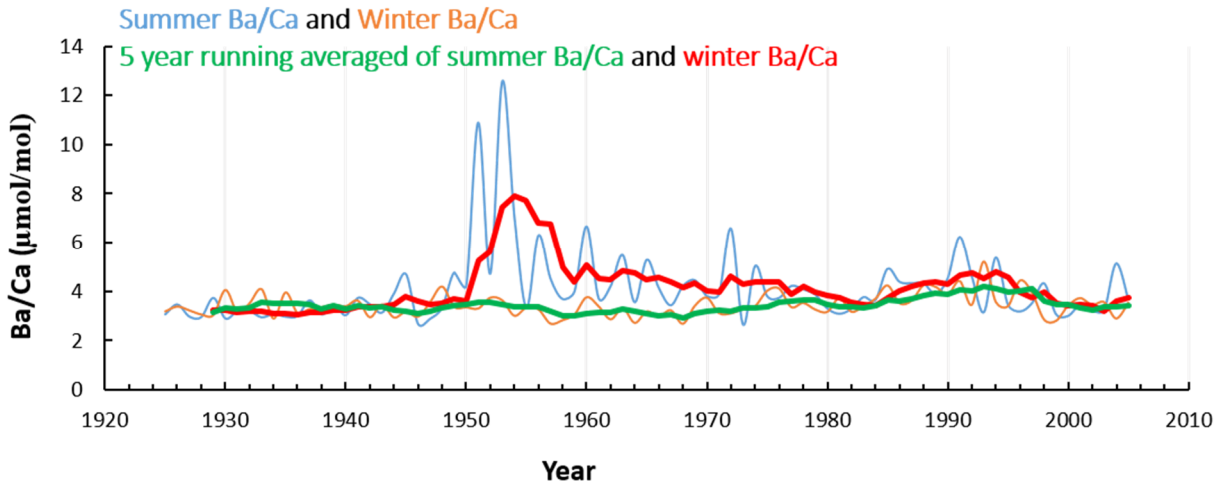

Figure 4.3. Comparison between summer Ba/Ca (July to September) and winter Ba/Ca (January to March) of Porites coral from Con Dao island during period 1924 to 2005.

In period from 1924 to 2005, the Ba/Ca ratios in summer is quite stable with range from 2-4 μmol/mol (Figure 4.3). The winter Ba/Ca was similar but there was an apperance of large peak in 1950s, indicated the increasing of Ba concentration in coral. This could be explained by the increasing of suspended sediment discharge from Mekong river related to land uses changes or the Indochina wars in that time.

I tried to devided the variation of Ba/Ca ratios into 3 stages using the Indochina wars period as reference. The first stage (before Indochina wars) showed relatively stable ratios from 1924 to 1945, with most Ba/Ca ratios varying between 2 and 4 μmol mol^{-1}, with the exception of a high value in 1933 and 1935. In the second stage (Indochina wars) from 1946 to 1975, Ba/Ca ratios showed an increasing trend with the maximum value in 1953, in addition there is the appearance of abnormal peaks in the winter. The third stage (After Indochina wars and Starting of Hydropower dams construction) from 1976 to 2005, with an increasing trend from 1980 to 1997 and a little decreasing from 1998 to 2005. But in this third stage, the abnormal peaks also occurred in winter. The mean values of the three stages were 3.294, 3.754 and 3.683 μmol mol^{-1}, respectively. The standard deviations of the three stages were 0.437, 1.726 and 0.850 μmol mol^{-1}, respectively, which indicated that the amplitude of the variation is increasing in the second stage.

The maximum peak of Ba/Ca usually occur in winter (Demcember to April) but sometimes it shows 2 peaks in one year, one peak in winter and other one in summer which indicate for flood events. We calculated the averaged value of Ba/Ca ratios in summer month of the flood year in period from 1980 to 2005. The averaged value was 3.6 μmol/mol. We also calculated this value for each year in period from 1924 to 1979. We found that in 1926, 1930, 1933, 1935, 1948, 1952, 1960, 1961, 1975, 1976, 1978 the averaged Ba/Ca value in summer month is similar 3.6 μmol/mol, especially in 1948 and 1960 with 4.23 and 4.25 μmol/mol, respectively. This means the flood events can be occurred in those years (Figure 4.1).

2. Reflection of EAM variablity on coral Ba/Ca and δ^{18}Osw records

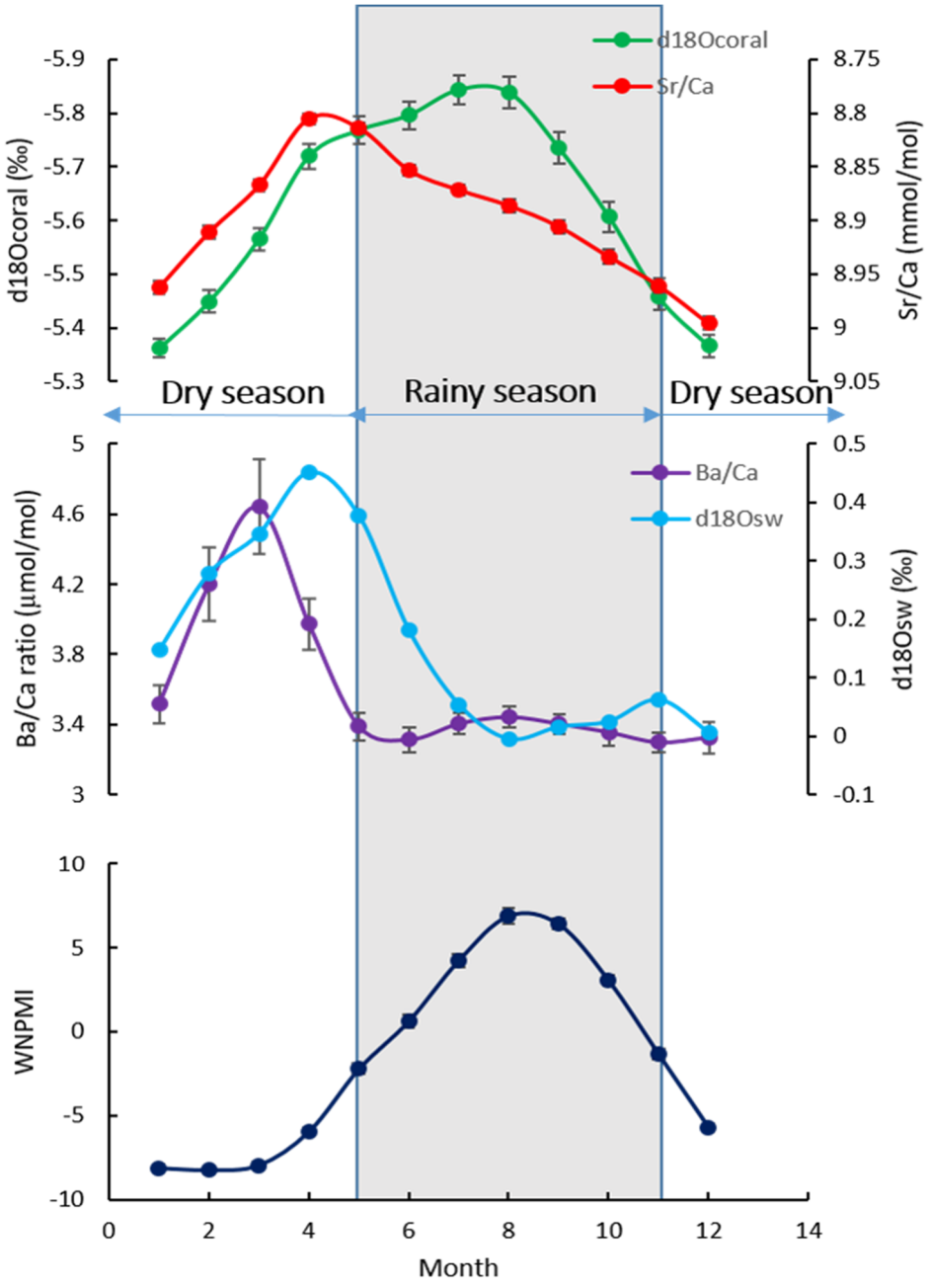

Figure 4.4. Seasonal characteristics of Sr/Ca, δ^{18}Oc, δ^{18}Osw, Ba/Ca and West Northern Pacific monsoon index (WNPMI) in period (1924-2005)

I calculated seasonal characteristic and compared between Sr/Ca, δ^{18}Oc, δ^{18}Osw, Ba/Ca and West Northern Pacific monsoon index (WNPMI) in period (1924-2005), where WNPMI showed that southwest monsoon is strong from July to September and reach maximum in August; the northeast monsoon is strong from Jan to March (Figure 4.4). I found that minimum values of $\delta^{18}O_{seawater}$ appeared in August correspond to maximum values of WNPMI (strong southwest

monsoon), in rainy season. And maximum values of Ba/Ca ratio occurred in March correspond to negative values of WNPMI (strong northeast monsoon), in dry season. This suggests Ba/Ca ratio and $\delta^{18}O_{seawater}$ recorded by Porites coral in Con Dao island can be used as proxy for northeast monsoon and southwest monsoon, respectively.

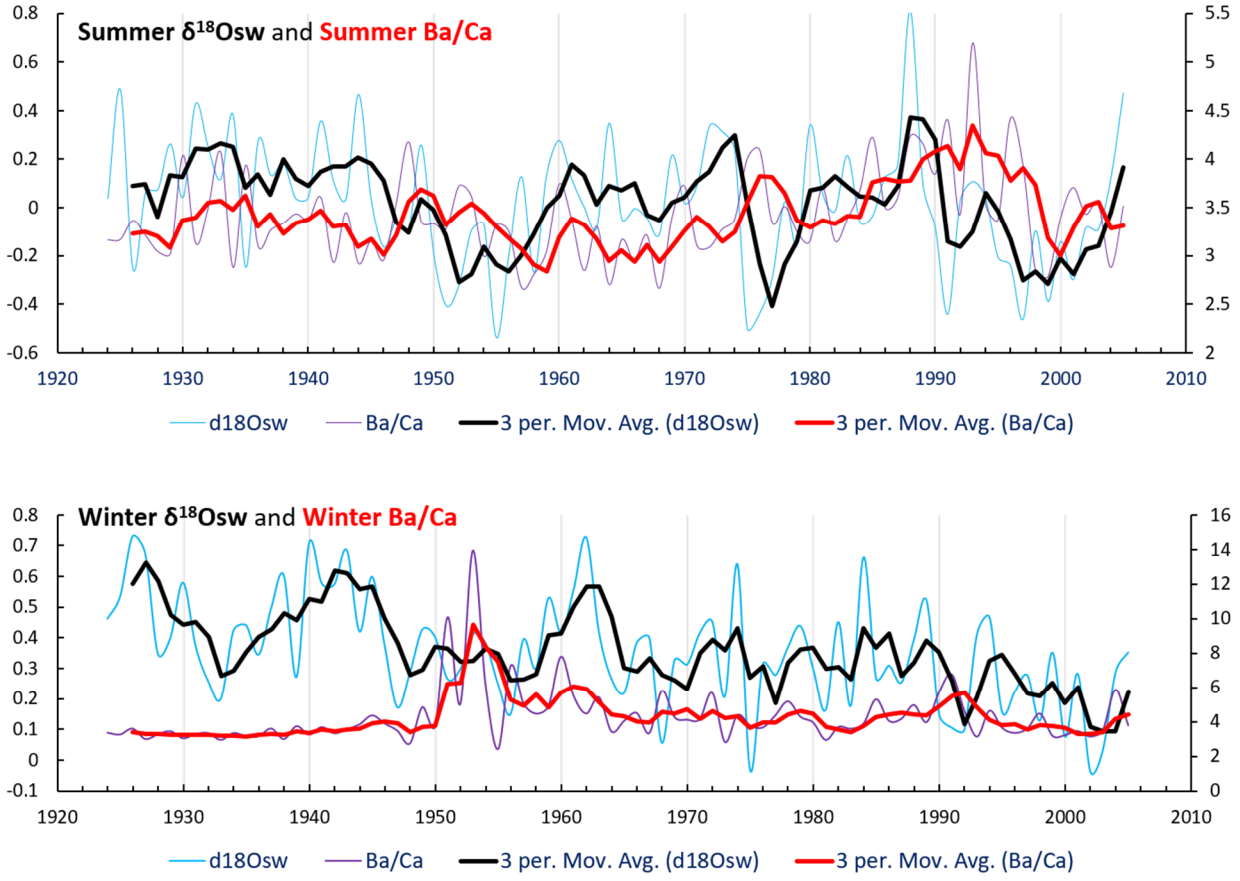

Figure 4.5. Comparison between seasonal averaged of coral Ba/Ca ratio and $\delta^{18}O_{seawater}$ in period from 1924 to 2005. (a) In summer (July to Septemeber); (b) In winter (January to March). Running averaged 3-year of each record was shown.

In summer, Mekong river discharge is controlled by EASM. Ba/Ca ratio seems to oscillate with δ^{18}Osw but probably increase since 1970s suggested the increase of suspended sediment discharge from Mekong River and the weakening of EASM. In winter, there was no correlation between Ba/Ca ratio and δ^{18}Osw. The range of variation and values of winter δ^{18}Osw tend to decrease through 82 years. This suggested the strengthening of EAWM associated the increasing of precipitation or fresh water runoff from Mekong river to Con Dao island.

References

1. Costenbader, John & Varns, Theo & Vidal, Adriana & Stanley, Lauren & Broadhead, Jeremy. (2015). Drivers of Deforestation in the Greater Mekong Subregion: Regional Report. 10.13140/RG.2.1.2992.5523.

2. Cropper, M., Griffiths, C., & Mani, M., 1999. "Roads, Population Pressures, and Deforestation in Thailand, 1976-1989" in Land Economics, 75(1), 58–73.

3. FAO, 2015. Global Forest Resources Assessment 2015: Desk Reference.

4. García-Ruiz, J.M., 2010. The effects of land uses on soil erosion in Spain: a review. *Catena*, 81, pp. 1-11.

5. Gupta, A. and S. C. Liew (2007), The Mekong from satellite imagery: A quick look at a large river, Geomorphology, 85, 259–274.

6. History of Vietnam Communist Party. In Vietnamese. Published 2008. National Political Publishing House, 768p.

7. McDonald, M.A., Healey, J.R., and Stevens, P.A., 2002. The effects of secondary forest clearance and subsequent land-use on erosion losses and soil properties in the Blue Mountains of Jamaica. *Agriculture Ecosystem Environment*, 92, pp. 1–19.

8. Milliman, J. D., and J. P. M. Syvitski (1992), Geomorphic/tectonic control of sediment discharge to the ocean: the importance of small mountainous rivers, The Journal of Geology, 525–544.

9. MRC, 2005b. Overview of the hydrology of the Mekong Basin. *Mekong River Commission.* (Available at: http://www.mrcmekong.org/. Accessed on: 21/12/2010).

10. MRC, 2006. MRC Annual Report 2006. *Mekong River Comission.*

11. MRC, 2009b. Initiative on sustainable hydropower work plan. Mekong River Commission. (Available at: http://www.mrcmekong.org/programmes/hydropower/hydropower-pub.htm. Accessed on: 17/12/2010).

12. Open Development Cambodia. 2015. “Forest Cover Study 1973-2014”. https://opendevelopmentcambodia.net/en/profiles/forest-cover/

13. Phimmavong, Somvang & Ozarska, Barbara & Midgley, Stephen. (2010). Forest and Plantation Development in Laos: History, Development and Impact for Rural Communities. International Forestry Review. 11. 501-513.

14. Turner, B.L. and Meyer, W.B. 1994. Global land-use and land-cover change: an overview. In: Changes in Land Use and Land Cover: A Global Perspective. Cambridge University Press, Cambridge, pp. 3-10.

15. Walling, D. E. (2008), The changing sediment load of the Mekong River. AMBIO, 37(3), 150–157.

16. Williams, G. P., and M. G. Wolman (1984), Downstream effects of dams on alluvial rivers, U.S. Geol. Surv. Prof. Pap. 1286, 83 pp.

Chapter 5

Coral Sr/Ca record and calculated δ^{18}Osw in Con Dao island as an indicator of ENSO and East Asian monsoon

Sea surface temperature (SST) records for tropical oceans provide an essential database for global climatic studies. Unfortunately, instrument-measured SST data are limited to a few decades and only available for limited locations (Fairbank et al., 1997). Therefore reconstruction of long-term paleo-SST records becomes very important. The Sr/Ca ratio from corals has been most widely accepted and used for tropical or subtropical paleo-SST reconstructions (e.g. Gagan et al., 1998; Corrège et al., 2005; Mitsuguchi et al., 2008). This will provide paleoclimatic records which are important for a better understanding of the dominent modes of the global climate system, such as: the El Niño-Southern Oscillation (ENSO) phenomenon of tropical Pacific origin, the East Asian monsoon, the Pacific Decadal Oscillation (PDO) and the mechanisms of decadal climate variability (Felis and Patzold, 2004).

Con Dao island located in East sea of Viet Nam area, is part of the tropical monsoon climate regime of Southeast Asia (Figure 5.1). From June to August, the region is affected by the Southwest Monsoon and tropical cyclones, which bring warm and wet tropical air masses to the study area, resulting in increased precipitation during the summer season. During the winter season from October to March, the region is influenced by the Northeast Monsoon, which brings cold and dry continental air to the study area. Episodic cold air outbreaks from the north can lead to anomalously low winter temperatures in the region. The climate of the this region is dominated by the East Asian monsoon (EAM) and can be related to the El Niño-Southern Oscillation (ENSO) owing to the interaction between ENSO and the EAM. ENSO is known as a periodic fluctuation (varying from 1 to 5 years) in SST (El Niño) and the air pressure of the overlying atmosphere (Southern Oscillation) across the equatorial Pacific Ocean. When an El Niño phase is mature in

boreal summer, the EASM is strengthened. When a mature phase of El Niño occurs in boreal winter, the EAWM is weakened. More recently, it has been shown that the EAWM is weakened (strengthened) in mature phases of El Niño (La Niña) (Huang et al., 2004). Moreover, the linkage between ENSO and West Pacific Warm Pool (WPWP) with mean annual SST ≥ 28 °C, could effect on sea surface temperature around Con Dao island. In the El Niño phase, the WPWP convection moves eastward along the equator to the central Pacific. In the La Niña phase, the WPWP convection is intensified in the western equatorial Pacific.

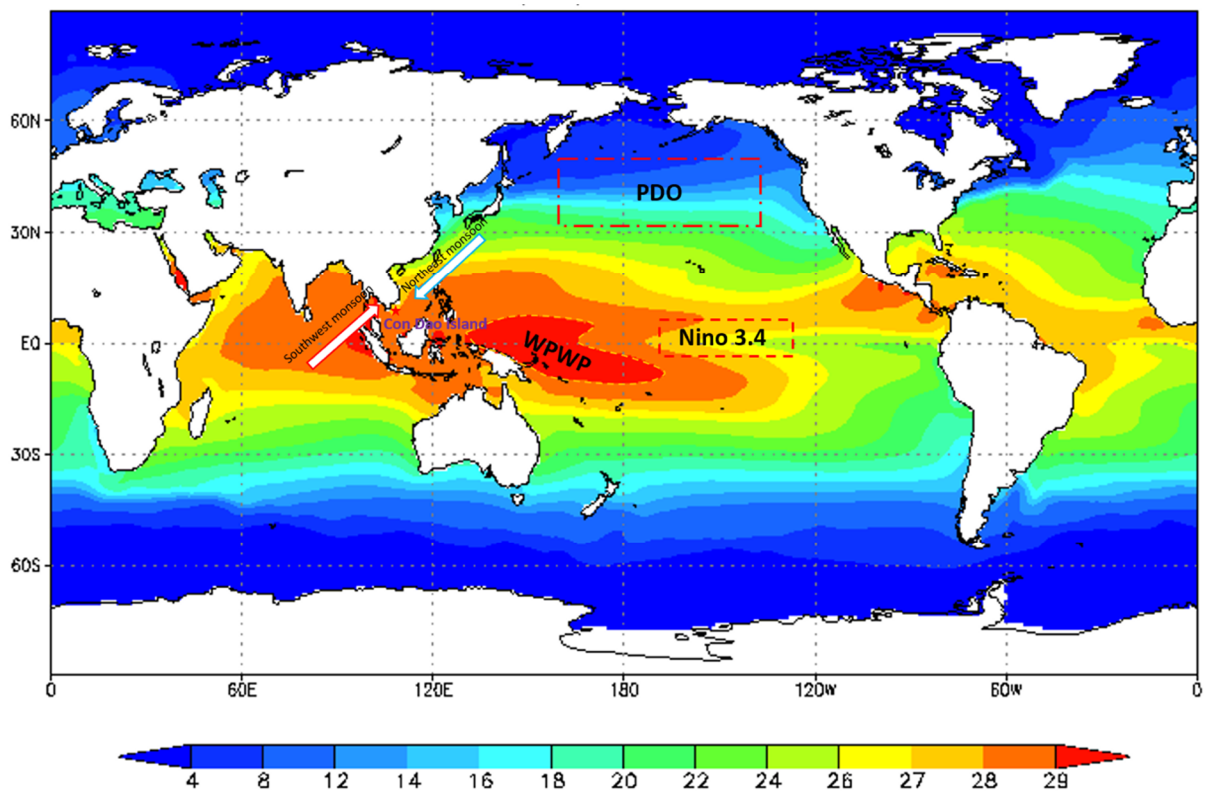

Figure 5.1. Distribution of sea surface temperature around Con Dao island. *Modified from Annual Mean Sea Surface Temperature (1982-1995) from National Weather Service Climate Prediction Center*

Monitoring of ENSO conditions primarily focuses on SST anomalies in region Niño 3.4 of the equatorial Pacific (from 170°W to 120°W longitude), and SST anomalies in this region are known as Niño 3.4 index. The coral Sr/Ca ratios from Con Dao island showed good correlation with instrumental SST (r = - 0.90) and the variation corresponds to SST, this indicated that the

Sr/Ca data primarily reflects seasonal SST variation in Con Dao island. For examination the correlation between my data with ENSO, I compared between annual average values of Sr/Ca and Niño 3.4 index during the period from 1924 to 2005. The result showed the positive correlation between summer Sr/Ca and Nino 3.4 index from 1924 to 1990 with correlation coefficient r = 0.516 and r = 0.725 corresponding to winter and summer, respectively. It suggested that Porites coral in Con Dao island can record ENSO variability from 1924 to 1990. However, from 1990 Nino 3.4 index and summer Sr/Ca are almost opposite (Figure 5.2).

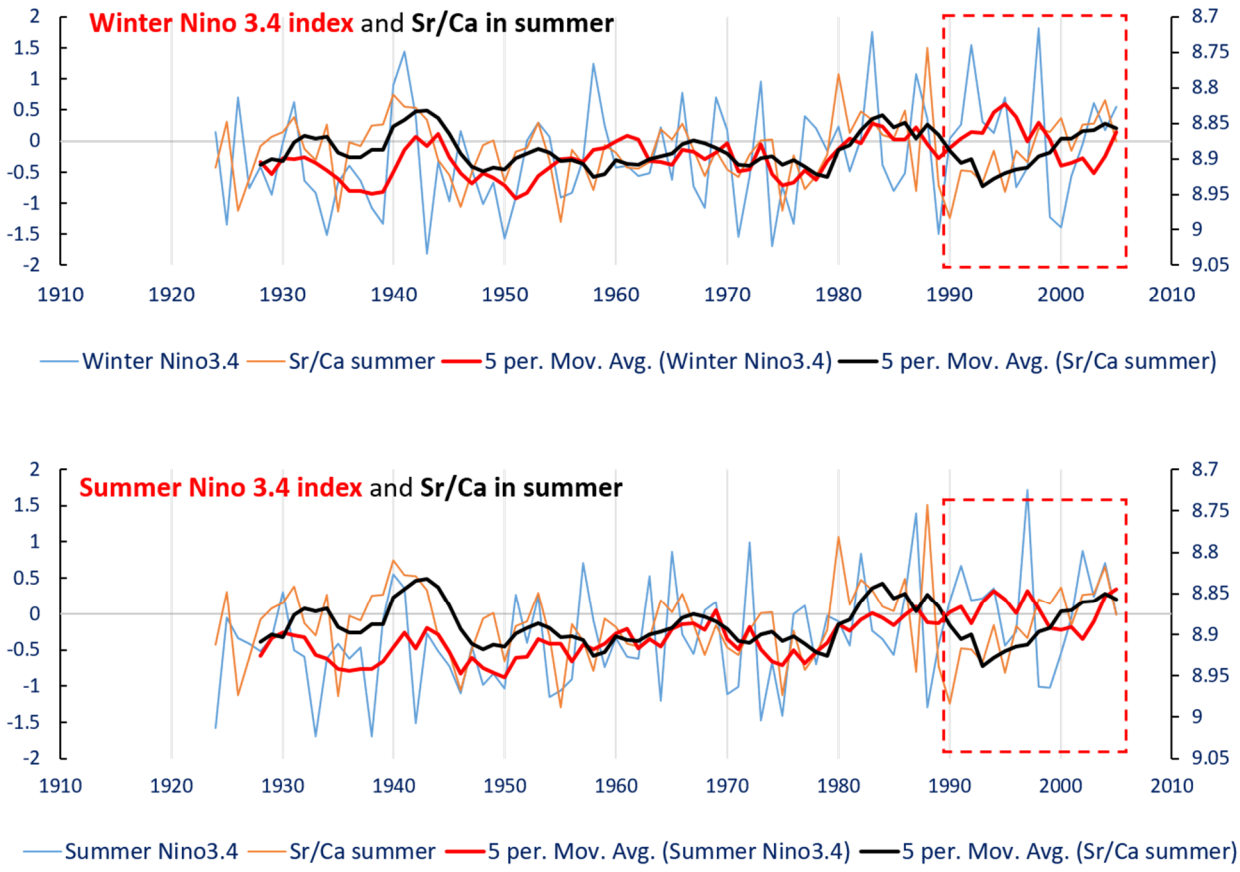

Figure 5.2. Comparison between summer Sr/Ca ratio from Porites coral in Con Dao island and Nino 3.4 Index during period from 1924 to 2005.

To explain for the difference between summer Sr/Ca and Nino 3.4 index from 1990, I thought that coral Sr/Ca ratio can be effected by local factors. In southern Vietnam, precipitation suddenly increases in the summer, when 80–90% of the annual discharge of the Mekong River occurs. The river discharge associated phytoplankton blooms ("vital effect") were demonstrated effect on coral in Con Dao island (Tang et al., 2006). These environmental conditions are likely to disturb coral physiological processes (i.e., stress on corals, increase of nutrients, change in light intensity) may lead to disturbance of Sr/Ca in coral. It has been suggested that coral Sr/Ca is

effected by coral physiological variations (Marshall and McCulloch, 2002). Other factor was considered may effect on coral Sr/Ca in Con Dao island. It is eruption of mount Pinatubo, Philippines. It occurred on June 15, 1991 and recorded as the second-largest volcanic eruption of this century. The effect from this eruption was nearly 20 million tons of sulfur dioxide were injected into the stratosphere, and dispersal of this gas cloud around the world caused global temperatures to drop temporarily (from 1991 to 1994) by about 0.5 °C. The distance from Con Dao island to mount Pinatubo is about 1500 km (Figure 5.3). The dispersal of sulfur dioxide effect on light intensity to the ocean and effect on photosynthesis process of corals lead to changes responses of corals with sea surface temperature at that time.

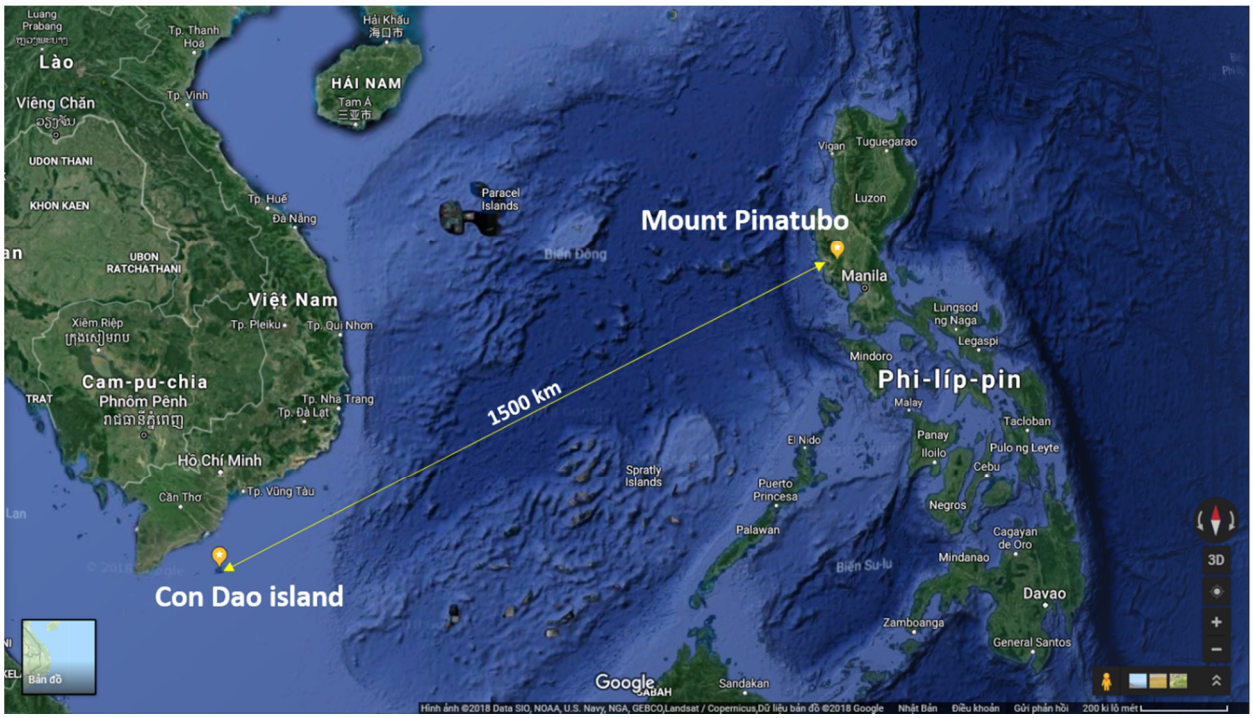

Figure 5.3. Location of Con Dao island and Mount Pinatubo

Our analytical results also show that coral $\delta^{18}O$ ($\delta^{18}Oc$) have very clear annual cycles similar to SST record, indicate that $\delta^{18}Oc$ was effected by SST. However, $\delta^{18}Oc$ is influenced by both SST and the $\delta^{18}O$ in seawater. At our study site, the mean seasonal variation in SSS was approximately 6 ‰, with a maximum of 34 ‰ in February - April and a minimum of 28 ‰ in October. Therefore, $\delta^{18}Osw$ might be a significant contribution to coral $\delta^{18}O$. $\delta^{18}O_{sw}$ values was calculated from both the coral Sr/Ca ratio and $\delta^{18}O_c$. To isolate $\delta^{18}O_{sw}$, the SST component was removed from the $\delta^{18}O_c$ values using Sr/Ca-SST estimates (Cahyarini et al., 2014). $\delta^{18}O_{sw}$ can be used as a good proxy for sea surface salinity (Watanabe et al., 2003). Like SST, sea surface salinity (SSS) is an extremely important physical parameter in climate studies. Together with temperature,

salinity is the driving force of the thermohaline circulation. Salinity also plays a crucial role in the generation of ENSO events. And because changes in SSS can often be related to changes in precipitation/ evaporation regimes, a good tracer of salinity has the potential to give information on atmospheric components of climate.

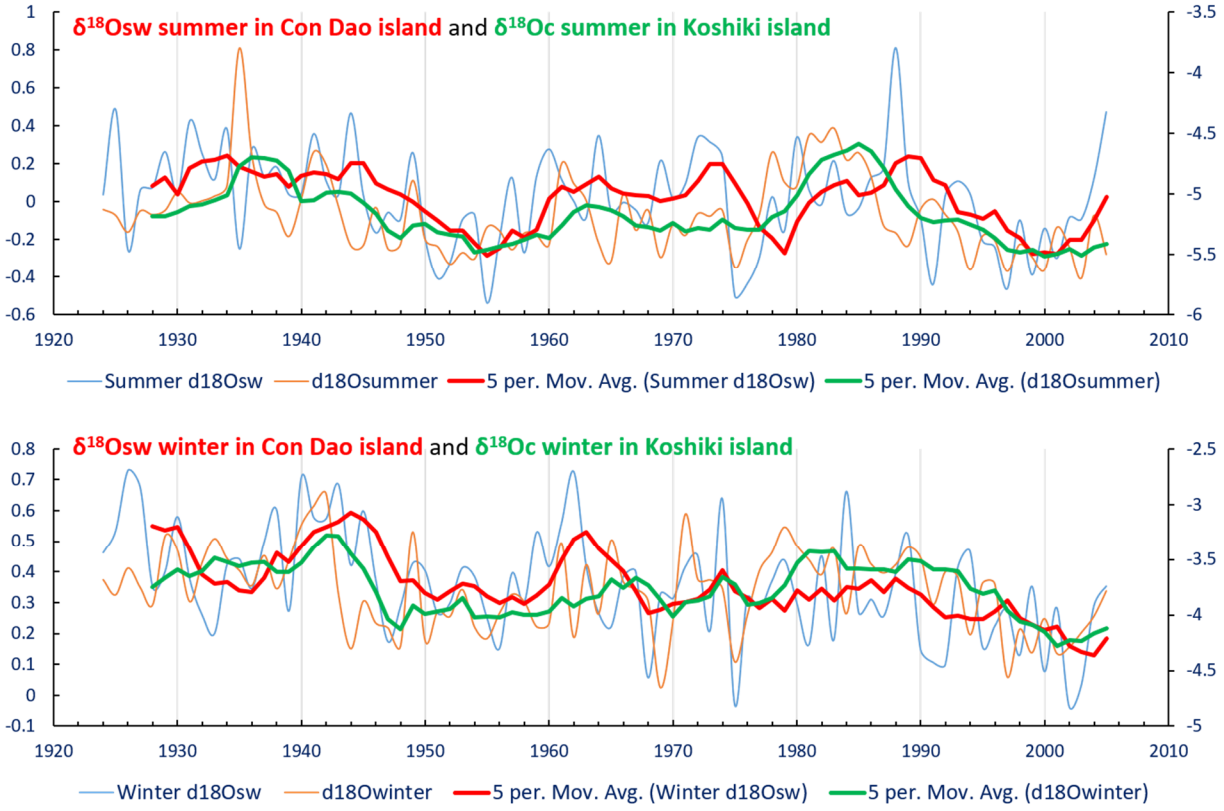

Figure 5.4. Comparison between δ^{18}Osw in Con Dao island, Viet Nam and δ^{18}Oc in Koshiki island, Japan. Running averaged 5 year showed good correlation between them.

Koshiki island is in the East China Sea, which is located 38 km west of the port city Ichikikushikino, Kagoshima, Japan. This island was influenced by EAM and the Changjiang River discharge significantly influenced on SSS around Koshiki island (Watanabe et al., 2014). The location of Koshiki island have similar conditions with my study area. δ^{18}O of Porites coral from Koshiki island was measured in research of Watanabe et al., 2014. Their result showed good correlation between δ^{18}O and Pacific Decadal Oscillation (PDO) and suggested that the East Asian

summer monsoon (EASM) may act as the driving force of winter PDO variability. I tried to compared δ^{18}Osw from Con Dao island with δ^{18}Ocoral from Koshiki island. And I found that the significant correlation between δ^{18}Osw in Con Dao island and δ^{18}Oc in Koshiki island with correlation coefficient are r = 0.52 and r = 0.60 corresponding to summer and winter, respectively.

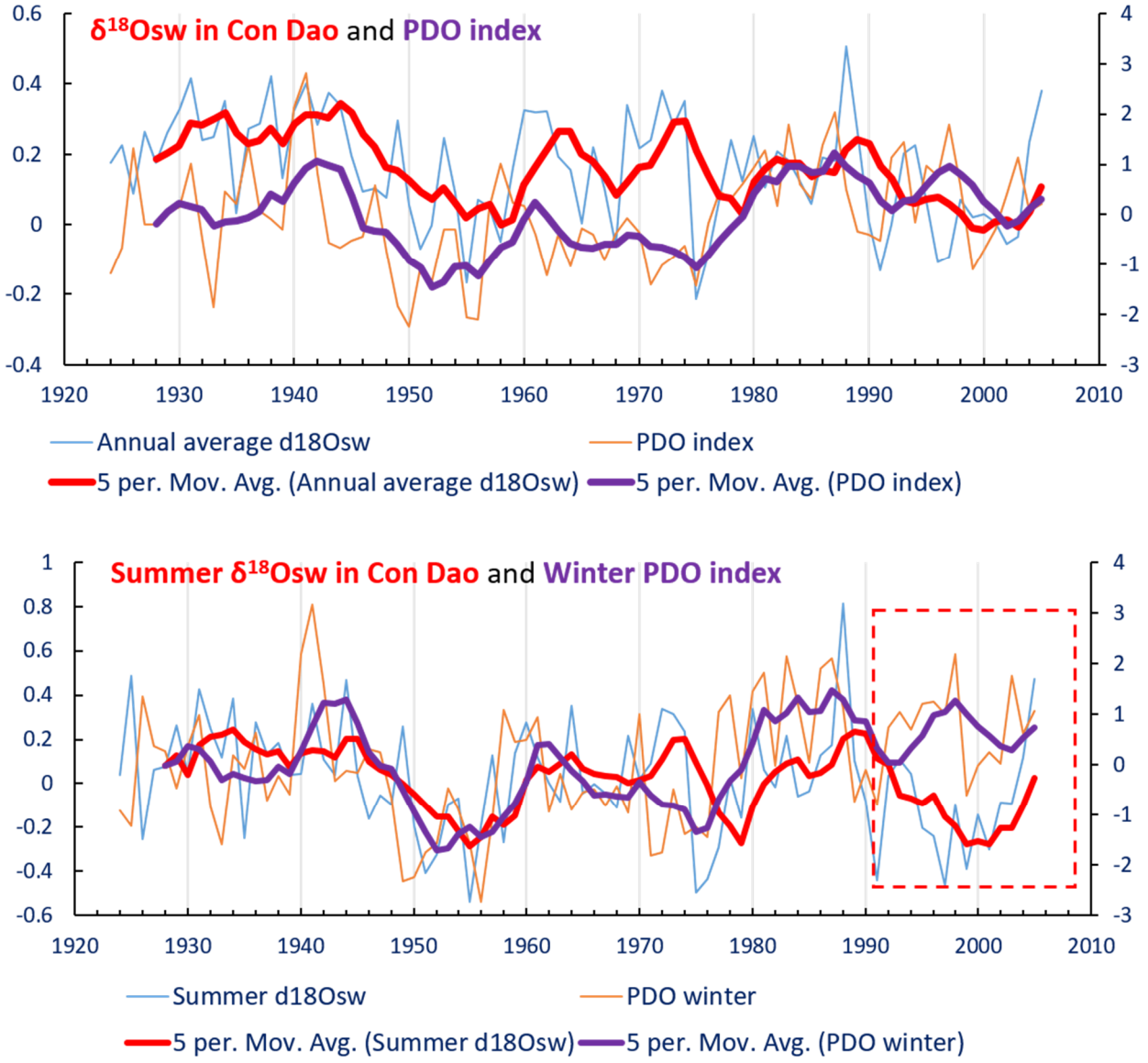

Figure 5.5. Comparison between δ^{18}Osw in Con Dao island and PDO index

The 5 year moving average profile of Con Dao island δ^{18}Osw was significantly correlated with the PDO index, demonstrating that the PDO was teleconnected in the ESVN during the last 82 years. The good correlation between the summer coral record and the winter PDO index suggesting that the EASM may be a possible driving force of winter PDO variability in this region

in period from 1924 to 1990. The difference from 1990 can be explained similar the difference between coral Sr/Ca and Nino 3.4 index. Moreover, δ^{18}Osw was isolated from δ^{18}Oc and Sr/Ca, therefore it can be effected.

References

1. Fairbanks, R. G., M. N. Evans, J. L. Rubenstone, R. A. Mortlock, K. Broad, M. D. Moore, and C. D. Charles (1997), Evaluating climate in- dices and their geochemical proxies measured in corals, Coral Reefs, 16, S93–S100.
2. Gagan, M. K., L. K. Ayliffe, D. Hopley, J. A. Cali,G.E.Mortimer, J. Chappell,M.T. McCulloch, and M. J. Head (1998), Tempera- ture and surface-ocean water balance of the Mid-Holocene tropical western Pacific, Science, 279, 1014–1017.
3. Mitsuguchi, T., Dang, P.X., Kitagawa, H., Uchida, T., Shibata, Y. (2008) Coral Sr/Ca and Mg/Ca records in Con Dao Island off the Mekong Delta: Assessment of their potential for monitoring ENSO and East Asian monsoon. *Global and Planetary Change* 63, 341–352.
4. Correge, T., 2005. Sea surface temperature and salinity reconstruction from coral geochemical tracers. Palaeogeography, Palaeoclimatology, Palaeoecology 232, 408–428
5. Felis, T., Patzold, J. (2004). Climate Reconstructions from Annually Banded Corals. Global Environmental Change in the Ocean and on Land, Eds., M. Shiyomi et al., pp. 205–227.
6. Huang, R., Chen, W., Yang, B., Zhang, R., 2004. Recent advances in studies of the interaction between the East Asian winter and summer monsoons and ENSO cycle. Adv. Atmos. Sci. 21, 407–424.
7. Marshall, J.F., McCulloch, M.T., 2002. An assessment of the Sr/Ca ratio in shallow water hermatypic corals as a proxy for sea surface temperature. Geochim. Cosmochim. Acta 66, 3263–3280.
8. Cahyarini, S.Y., Pfeiffer, M., Timm, O., Dullo, W.C., Schönberg, D.G. (2008) Reconstructing seawater δ^{18}O from paired coral δ^{18}O and Sr/Ca ratios: methods, error analysis and problems,

with examples from Tahiti (French Polynesia) and Timor (Indonesia). *Geochimica et Cosmochimica Acta* 72, 2841–2853.

9. Tang, D.L., Kawamura, H., Shi, P., Takahashi, W., Guan, L., Shimada, T., Sakaida, F., Isoguchi, O. (2006) Seasonal phytoplankton blooms associated with monsoonal influences and coastal environments in the sea areas either side of the Indochina Peninsula. *Journal of Geophysical Research* 111, G01010, doi:10.1029/2005JG000050.

10. Watanabe, T., Gagan, M.K., Corrége, T., Gagan, H.S.,Cowley, J., Hantoro, W.S. (2003) Oxygen isotope systematics in Diploastrea heliopora: New coral archive of tropical paleoclimate. *Geochimica et Cosmochimica Acta* 67, 1349–1358.

Chapter 5.
CONCLUSIONS

My research has established monthly resolution geochemical records from an annually-banded Porites coral collected from Con Dao Island, ~90 km distance from the Mekong River mouth in the southern of ESVN in period from 1924 to 2005 for reconstructing past sea surface conditions, Mekong river discharge and East Asian monsoon variablity.

(1) The results showed the high correlation between Sr/Ca and instrumental SST ($r = 0.90$; $P < 0.01$). The differences between the reconstructed and observed SSTs were 0.45, -0.89 and -0.33 °C for annual maximum, minimum and mean values, respectively. The reconstructed SST in period from 1924 to 2005 is quite stable and the standard deviation of residuals of the regression was determined to be 1.45 °C due to differences in ocean conditions and SST between observation site and sampling site. For determining ENSO variability and its impacts to ESVN, I compared between coral Sr/Ca and Nino 3.4 index. I found that coral Sr/Ca ratios from 1924 to 1990 showed significantly correlation with Nino 3.4 index with correlation coefficient $r = 0.516$ and $r = 0.725$ corresponding to winter and summer, respectively. This result suggested that interannual variability SST around Con Dao island is strongly influenced by ENSO. From 1990 to 2005, relationship between Nino 3.4 index and summer Sr/Ca are almost opposite due to influence of Mekong river discharge or the eruption of Mount Pinatubo, Philippines.

(2) The time series of Ba/Ca is characterized with intra-annual double peaks, the first large one in March during the dry season and relatively small one in August during the wet season. Coral Ba/Ca record in Con Dao Island could reflect the sediment discharge from the Mekong River. The maximum discharge of freshwater from the river reached our coral site in summer (from May to November), however the sediment discharge model of the Mekong River indicated that the amount of suspended sediment influencing on Con Dao Island was high in winter (from December to April) because of the influence from the seasonal migration of the Asian monsoon and ocean currents. Coral Ba/Ca ratios can be used as reflection of the suspended sediment discharge from Mekong river in period 1924 to 2005 and divided into 3 stages: Before war (1924 to 1945), Indochina war (1946 to 1975) and After war and hydropower dams construction (1976 – 2005). The variability of Ba/Ca can be explained by human activities such as: land-use changes, hydropower dams construction and Indochina war.

(3) On the other hand, coral Ba/Ca ratio and $\delta^{18}O_{sw}$ could be used as indicators of flooding from the Mekong Delta. During the period from 1980 to 2005, the difference in seasonal characteristics of geochemical signals in flood years and no-flood years was detected. During the flood years, in the warm/wet season, the Ba/Ca ratios and $\delta^{18}O_{sw}$ data significantly increased and decreased, respectively. These results reflect the increase in the Mekong River freshwater discharge and the sudden increase of precipitation when floods occurred in warm/wet season. In period from 1980 to 2005, the averaged value of Ba/Ca ratios in summer months (May to November) of flood years was calculated as 3.6 µmol/mol. Based on this, 11 flood events can be detected by averaged value of Ba/Ca in summer months similar or higher than 3.6 µmol/mol in

1926, 1930, 1933, 1935, 1948, 1952, 1960, 1961, 1975, 1976, and 1978, especially expected big flood events in 1948 and 1960 with averaged Ba/Ca is 4.23 and 4.25 µmol/mol, respectively.

(4) Ba/Ca ratios and $\delta^{18}O_{sw}$ recorded by *Porites* coral in Con Dao island can be used as proxy for northeast and southwest monsoon, respectively. $\delta^{18}O_{sw}$ showed a high correlation with $\delta^{18}O$ in coral from Koshiki island which is also influenced by East Asian Monsoon. I found the significant correlation between $\delta^{18}O_{sw}$ and Pacific Decadal Oscillation (PDO) index, suggested that climate of ESVN was teleconnected with decadal variation of Pacific Ocean during the last 80 years. High correlation between summer $\delta^{18}O_{sw}$ and winter PDO index during 1924 to 1990 indicated that EASM may be a possible driving force of winter PDO variability. The no correlation between summer $\delta^{18}O_{sw}$ and winter PDO index from 1990 to 2005 corresponds with cooling event showed in the results of Sr/Ca variation.